



Jupiter
POWER

**Storage Made
Strategic.™**

Attachment E-3: Trimount Energy CFD Report

Pictured: Jupiter's Callisto | BESS in Harris County, TX

Prepared For:

Massachusetts Department of Energy Resources

Electric Distribution Companies:

Fitchburg Gas & Electric Light Company d/b/a Unitil

Massachusetts Electric Company and Nantucket Electric Company,
each d/b/a National Grid

NSTAR Electric Company d/b/a Eversource Energy

Applicant Information

Applicant:

Trimount ESS LLC

Contact:

Sam Malin
Vice President, Origination
sam.malin@jupiterpower.io
(512) 541-5240

Ford Martin
Associate, Origination
ford.martin@jupiterpower.io
(512) 629-6179

Address:

1108 Lavaca St, Suite 110-349
Austin, TX 78701



Jupiter Power LLC

Trimount ESS LLC
Computational Fluid Dynamics Heat Flux and Fixed Water
Spray Modeling Proof of Concept Report
Trimount Energy Storage
Everett, Massachusetts

FINAL REPORT / REV2 / October 2024



Prepared for:
Trimount ESS LLC
Everett, MA

Prepared by:
Fire & Risk Alliance, LLC.
7640 Standish Place
Derwood, MD 20855

www.fireriskalliance.com

301-658-3060

The distribution of this document to third parties is prohibited without written approval from Fire & Risk Alliance, LLC.



10/02/2024	REV2	Final	KS	MK	MK
09/12/2024	REV 1	Final	KS	MHR	MHR
08/30/2024	REV 0	Draft	KS	MHR/MK	MHR
Date	Revision	Reason for Issue	Developed By	Checked By	Approved by

REVISION CONTROL SHEET

REVISION	SECTION	CHANGE NOTED
Rev2	1.2, 2.1, 7.0	Updated Descriptive Language

EXECUTIVE SUMMARY

Fire & Risk Alliance, LLC (FRA), was requested by Jupiter Power, LLC (Client) to conduct a Computational Fluid Dynamics (CFD) based proof of concept (POC) analysis for the Hithium 5.015 MWh Battery Energy Storage System (BESS) double stack arrangement for the Trimount Energy Storage project.

PURPOSE

The primary purpose of this analysis was to evaluate the incident heat flux and temperature impacts for the double stack BESS arrangement, from a fully involved fire occurring in an initiating BESS unit on the lower level, to adjacent BESS containers (vertically stacked and across the aisle) and structural members. The analysis included CFD simulations with and without exterior fire suppression to provide a POC analysis for the double stack arrangement and external fire suppression system.

SCOPE

The scope of this analysis was limited to evaluating a single double stack arrangement and structural support design as provided by the Client. This analysis examines the potential for propagation between initiating and target BESS containers and evaluates exposure conditions for impacted structural members. It is understood, the predicted thermal boundary conditions at the structural members will be utilized to develop an improved structural design to withstand the predicted fire exposure conditions based on the specific structural loads. Further structural design and load specific analysis is outside of the scope of the analysis documented in this report.

CFD APPROACH

The CFD program FDS (Fire Dynamics Simulator) was used to model a fully involved Hithium BESS fire both with and without activation of the proposed automatic water spray system to determine and report the external heat flux and surface temperature impacts to target BESS containers and to representative structural steel members at steady state conditions. The calculated external heat flux was then applied to a small scale 1D heat transfer model to determine the peak internal module surface temperatures for target BESS due to worst-case external heat flux conditions.

RESULTS

Two scenarios were evaluated, one without any exterior fire protection and one with an exterior fixed water spray system. The results showed that without any exterior fire protection target BESS and structural members are constantly exposed to average maximum temperatures and heat flux values in excess of 700°C and 70 kW/m² respectively with peaks up to 100% greater experienced for ~7% of the fire duration. The results with the water spray system demonstrated that the water spray system is able to significantly reduce the average maximum exterior heat flux and temperature values such that the average maximums are 30 kW/m² and 150 °C respectively. Additionally, instantaneous peaks of 55 kW/m² and 584 °C are experienced for ~3% of the fire duration. Figure ES.1 shows temperature results for representative structural

members and target BESS (T3) for Scenario 1 (without external fire suppression) and Scenario 3 (with external water spray system). The results show that the water spray system is able to significantly reduce the temperature (and non-pictured heat flux) impacts to the structure and target BESS.

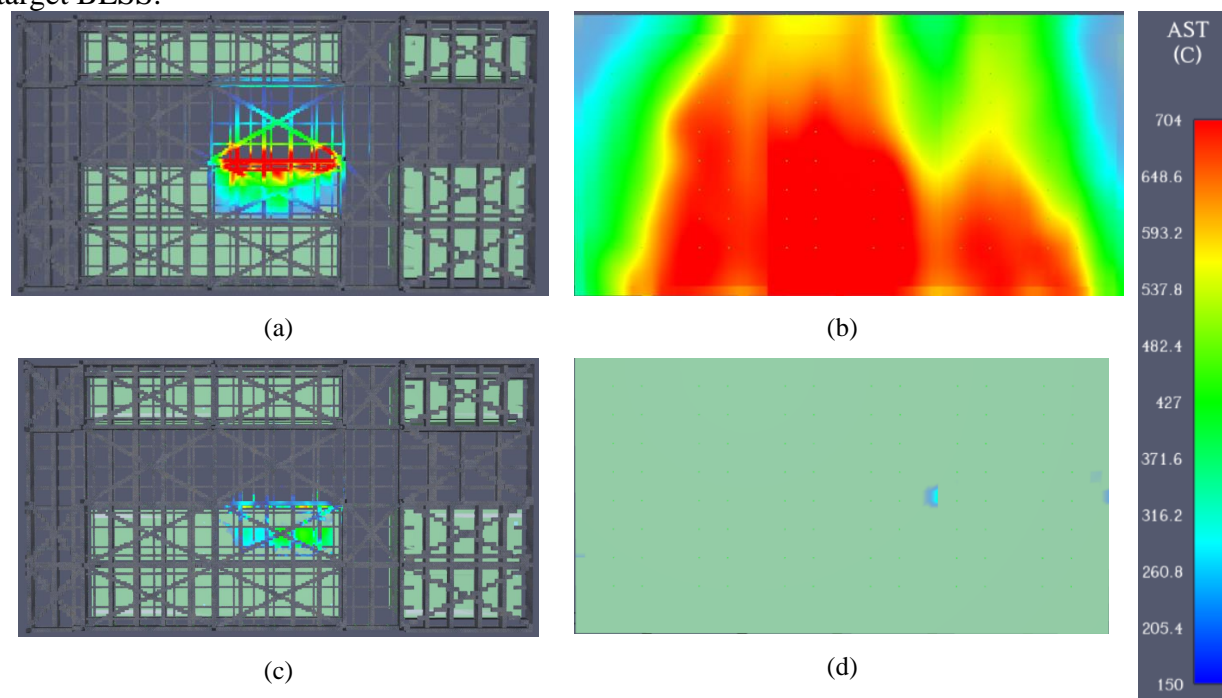


Figure ES.1. Temperature results visualization (a) Scenario 1 structural, (b) Scenario 1 T3 front, (c) Scenario 3 structural, (d) Scenario 3 T3 front

The 1D heat transfer models found that without any exterior fire protection, module surface temperatures exceed the cell venting temperature when exposed to the average maximum external heat flux values, representative of 93% of the fire duration and exceed the cell thermal runaway temperature when exposed to the instantaneous peak external heat flux values, representative of ~7% of the fire duration. With the addition of the exterior fixed water spray system, module temperatures reach a steady state value of less than 160 °C which provides a 25% safety factor to the cell venting temperature and a 75% safety factor to the cell thermal runaway temperature. Figure ES.2 shows the maximum module temperature for each scenario for comparison.

CONCLUSIONS

An external water spray system is required to prevent thermal runaway propagation between BESS units for a fully involved BESS fire on the lower level. Additionally, the water spray system is able to significantly reduce both the duration and intensity of the incident heat flux and temperature experienced at the steel structure. The current analysis shows that this is a feasible solution as the water spray system provides cooling to the structure and adjacent containers preventing fire propagation to containers above and adjacent. Further structural analysis will confirm the feasibility of this design as it progresses.

TABLE OF CONTENTS

1.0	INTRODUCTION	1
1.1	Objectives	1
1.2	Scope.....	1
2.0	METHODOLOGY AND APPROACH.....	3
2.1	Evaluation Criteria	3
2.2	Fire Dynamic Simulator.....	4
2.3	Smokeview	4
3.0	FDS MODELING SCENARIOS.....	5
4.0	HEAT FLUX FIRE MODEL INPUTS (SCENARIOS 1 & 3)	6
4.1	Design Fire Development	6
4.1.1	UL 9540A Summary.....	6
4.1.2	Design Fire Basis	6
4.2	Design Fire Inputs.....	6
4.3	CFD Model Geometry	7
4.3.1	Hithium BESS Geometry.....	7
4.3.2	Structural Geometry	9
4.4	External Fire Suppression Nozzle Model (scenario 3 only).....	10
4.5	Extinction Model	11
4.6	Grid Size	12
4.7	Ambient Conditions.....	12
4.8	Simulation Duration	13
5.0	1D HEAT TRANSFER MODEL INPUTS (SCENARIOS 2 & 4).....	14
5.1	BESS Geometry	14
5.2	Boundary Conditions.....	14
5.3	Other Model inputs	16
6.0	FDS MODEL RESULTS & ANALYSIS	17
6.1	Scenario 1.0 Results (0 wind)	18
6.1.1	T3 time dependent heat flux analysis.....	20
6.1.2	Structural members time dependent temperature analysis	21
6.2	Scenario 2.0 Results (0 wind)	22
6.3	Scenario 3.0 Results (0 wind)	24

6.3.1	T3 time dependent heat flux analysis	27
6.3.2	Structural members time dependent temperature analysis	27
6.4	Scenario 4.0 (0 wind)	28
6.5	Results and Analysis Summary	29
7.0	CONCLUSION	33
8.0	REFERENCES	34

LIST OF FIGURES

Figure 1. Hithium BESS container configuration; (a) exterior, (b) interior	8
Figure 2. FDS model of Hithium BESS (front view of initiating unit)	9
Figure 3. CAD drawing of Trimount Energy Storage double stack site arrangement.....	9
Figure 4. Trimount Energy Storage double stack model domain; (a) iso-view, (b) side view	10
Figure 5. Plan (left) and section (right) view of water spray nozzle arrangement.....	11
Figure 6. 1D heat transfer FDS model domain	14
Figure 7. Scenario 2 applied external heat flux (1D heat transfer without external water spray)	15
Figure 8. Scenario 4 external applied heat flux (1D heat transfer with external water spray)	15
Figure 9. FDS results nomenclature guide.....	18
Figure 10. 3D Smokeview visualization of smoke and heat.....	18
Figure 11. Integrated heat flux (a) at 12 kW/m ² ; (b) 30 kW/m ² [view C]	19
Figure 12. Incident heat flux at (a) View A, (b) View D, (c) View B, (d) View E	19
Figure 13. Surface temperature at (a) View A, (b) View D, (c) View B, (d) View E	20
Figure 14. Structural steel temperature results visualization	22
Figure 15. Scenario 2 internal target module surface temperature	23
Figure 16. worst case target module surface temperature.....	24
Figure 17. 3D Smokeview visualization of smoke and heat.....	25
Figure 18. Integrated heat flux (a) at 12 kW/m ² ; (b) 30 kW/m ² [view C]	25
Figure 19. Incident heat flux at (a) View A, (b) View D, (c) View B, (d) View E	26
Figure 20. Surface temperature at (a) View A, (b) View D, (c) View B, (d) View E	26
Figure 21. Structural steel temperature results visualization	28
Figure 22. Module surface temperature	29
Figure 23. Module surface temperature comparison	32
Figure 23. Schematic of Cell Layout and External Heaters for Module Level Test	37
Figure 24. Unit level test setup	38

LIST OF TABLES

Table 1. FDS scenarios summary table.....	5
Table 2. Design fire FDS inputs	7
Table 3. FDS model material properties [1,7,8]	8
Table 4. FDS nozzle model inputs.....	11
Table 5. FDS scenario 1 & 3 model ambient conditions	12
Table 6. FDS scenario 2 & 4 model ambient conditions	16
Table 7. Scenario 1: time dependent heat flux analysis.....	21
Table 8. Time dependent structure temperature results summary	22
Table 9. Scenario 3: time dependent heat flux analysis.....	27
Table 10. Time dependent structure temperature results summary	28
Table 11. Comparative time dependent heat flux analysis for T3 exterior.....	30
Table 12. Constituent concentrations based on cell level test data.....	35
Table 13. Cell failure temperatures.....	36

LIST OF ACRONYMS

Battery Energy Storage System	BESS	Initiating Unit	I
Jupiter Power, LLC	Client	Proof of Concept	POC
Computational Fluid Dynamic	CFD	National Institute of Science and Technology	NIST
Fire Dynamic Simulator	FDS	Smokeview	SMV
Fire & Risk Alliance	FRA	Target Unit 1/2/3	T(1/2/3)

1.0 INTRODUCTION

Fire & Risk Alliance, LLC (FRA), was requested by Jupiter Power LLC (Client) to conduct a Computational Fluid Dynamics (CFD) based proof of concept (POC) analysis for the Hithium 5.015 MWh Battery Energy Storage System (BESS) double stack arrangement for the Trimount Energy Storage project. The primary purpose of this analysis was to evaluate the incident heat flux and temperature impacts for the double stack BESS arrangement, from a fully involved fire occurring in an initiating BESS unit on the lower level, to both the adjacent BESS containers (vertically stacked and across the aisle) and structural members. The analysis included CFD simulations with and without exterior fire suppression to provide a POC analysis for the double stack arrangement and external fire suppression system.

FRA performed simulations using the Fire Dynamics Simulator (FDS) computational fluid dynamics (CFD) model of a fully involved BESS cabinet (6 racks of 8 modules). A flaming event from ignition of battery vent gas releases from involved BESS modules was simulated and the subsequent analysis evaluated the heat transfer and thermal boundaries for BESS, other electrical equipment, structures, and personnel at site.

1.1 Objectives

The main objectives of this analysis were:

1. To conduct CFD modeling of a fully involved fire in the initiating BESS *without activation of the proposed automatic water spray system*. Determine external heat flux and temperature impacts to target (non-initiating) BESS containers and structural supports from initiating BESS fire. Determine peak internal module surface temperatures for target BESS due to worst-case external heat flux conditions.
2. To conduct CFD modeling of a fully involved fire in the initiating BESS *with activation of the proposed automatic water spray system*. Determine external heat flux and temperature impacts to target (non-initiating) BESS containers and structural supports from initiating BESS fire. Determine peak internal module surface temperatures for target BESS due to worst-case external heat flux conditions.
3. Validate the fixed water spray design density proposed to prevent thermal runaway propagation to target BESS containers.
4. Provide a fire protection design proof of concept (POC) analysis for the Hithium double stack arrangement.

1.2 Scope

The scope of this analysis was limited to evaluating a single double stack arrangement and structural support design as provided by the Client. This analysis examines the potential for propagation between initiating and target BESS containers and evaluates exposure conditions for impacted structural members. The current analysis shows that this is a feasible solution as the water spray system provides cooling to the structure and adjacent containers preventing fire propagation to containers above and adjacent. Further structural analysis will confirm the feasibility of this design as it progresses. Further structural design and load specific analysis is outside of the scope of the analysis documented in this report.

CFD Analysis

The model utilized in this analysis includes a representative portion of the domain which can be applied to the entire site installation. This analysis is limited to evaluating the impact of a single representative fixed water spray system based upon the proposed fixed water spray system design density and coverage area. This analysis is anticipated to be used as a POC for the design phase, the details of the design being determined at a future date. Once the design is finalized, an additional model simulation should be run to verify the final design conditions.

2.0 METHODOLOGY AND APPROACH

The following steps were used to complete this analysis:

1. **Evaluation criteria development (Section 2.1):** Evaluation criteria are threshold values which are used to evaluate the results of an analysis.
2. **Design fire development (Section 4.1):** A representative design fire was developed based on UL 9540A test data, literature data, and previous experience.
3. **External heat flux analysis (Section 6.1):** The CFD program FDS was used to model a fully involved Hithium BESS fire to determine and report the external heat flux and surface temperature impacts to target BESS containers and representative structural steel members at steady state conditions.
4. **1D heat transfer analysis (Section 6.2):** The external heat flux calculated in step 4 is applied to a small-scale high-resolution model to determine the equilibrium temperature of module surfaces within target BESS for a long duration exposure.
5. **External heat flux analysis (with water spray system) (Section 6.3):** Step 4 is repeated with the addition of the external fixed water spray system to determine and report the external heat flux and surface temperature impacts to target BESS and representative structural steel members including cooling effects from the fixed water spray system
6. **1D heat transfer analysis (with water spray system) (Section 6.4):** Step 5 is repeated with the updated external heat flux values including cooling effects from the external fixed water spray system.

2.1 Evaluation Criteria

Evaluation criteria are threshold values that if exceeded indicate an unacceptable level of damage may occur to targets (i.e. target BESS & structural steel). Evaluation criteria are required to be specified to evaluate performance-based designs to ensure an acceptable performance of the system. Due to the unique nature of the proposed installation, the fire protection design follows a performance-based approach with a goal of minimizing the impact of a large-scale flaming event on both structural and equipment targets.

For this analysis, the desired system performance is to prevent a fully involved BESS fire from propagating to adjacent containers (i.e. initiating fire event is limited to single involved BESS container) and to prevent structural steel failure. In order to prevent thermal runaway propagation, cells in target BESS must not exceed their critical venting or thermal runaway temperature as determined by the UL 9540A test. A critical cell venting temperature of **200.7 °C¹ (392 °F)** is used as the temperature threshold in this analysis, based on specific test data reported for the Hithium equipment.

Structural steel failure is dependent upon the structural load, member sizes, thermal exposure duration and intensity. This results in this report present the exposure duration and intensity of fire effects on representative structural members. The results are compared to representative industry standard temperature and heat flux criteria in ASTM E119 to provide a frame of reference for the results. The current analysis shows that this is a feasible solution as the water

¹ Minimum cell venting temperature based on UL 9540A cell level test data (report # CN23F118 001).

spray system provides cooling to the structure and adjacent containers preventing fire propagation to containers above and adjacent. Further structural analysis will confirm the feasibility of this design as it progresses.

2.2 Fire Dynamic Simulator

Fire modeling was conducted using the Fire Dynamic Simulator (FDS) computational fluid dynamics software package (version 6.7.0), which was developed by the Building and Fire Research Laboratory at the National Institute of Standards and Technology (NIST).

FDS simulates fire behavior in complex 3D environments such as buildings, equipment, and surrounding structures. FDS uses the Large Eddy Simulation (LES) technique to analyze fluid flows in fires. The LES technique separates fluid flow into two parts: the large-scale turbulence regime, which is computed directly from fluid motion equations, and the small-scale turbulence regime, which is estimated using a sub-grid model. This technique is ideal for modeling fire growth, smoke movement, and heat radiation, which are driven by large-scale structures in fluid flow. With over 500 peer-reviewed publications and over 20 years of continued development, FDS has been extensively validated and proven to be an effective tool for fire simulations.

CFD models, such as FDS, divide the model space into thousands or millions of tiny volumes or cells. Inside each cell's volume, variables such as gas temperature and velocity are considered uniform, changing only with time. The model then solves simplified "low Mach number" equations of fluid and energy flow for each cubic volume (cell) within the computational domain, thereby describing the large eddy fire phenomenon over all of the cubic volumes in the computational domain as a function of time.

The portions of the FDS code used to model various aspects of fire physics (e.g., fire growth and spread, smoke development and spread) have been rigorously tested against experimental data. These studies have dealt with areas involving fire growth and spread, suppression, and dispersion of smoke and hot gases throughout a large-scale environmental domain.

2.3 Smokeview

Smokeview (SMV), is a post processor which is developed by NIST and is used to analyze the outputs visually that are obtained from the FDS CFD solver. The FDS solver develops *.smv files which are then accessed using SMV software to analyze & present various results. Smokeview was used to generate the visual results provided in this report.

3.0 FDS MODELING SCENARIOS

Four primary modeling scenarios were included in this analysis:

- Scenario 1: External heat flux *without* external fixed water spray protection
- Scenario 2: 1D heat transfer *without* external fixed water spray protection
- Scenario 3: External heat flux *with* external fixed water spray protection
- Scenario 4: 1D heat transfer *with* external fixed water spray protection

Scenarios 1 and 3 include five variations each to evaluate wind impacts from both the four primary wind directions (north, south, east, and west) and under no-wind conditions. Scenarios 2 and 4 are based on the worst-case external heat flux results obtained from Scenarios 1 and 3, respectively, for the worst-case wind conditions (direction and speed). For both scenarios 1 and 3, the no wind conditions presented the worst-case exposure to target BESS.

The table below summarizes the simulation scenarios, variations, and associated inputs:

Table 1. FDS scenarios summary table

Scenario Identification #	Wind Direction	Wind Speed (MPH)	Nozzles	Initiating BESS doors
Scenario 1.0	n/a	0	no	open
Scenario 1.1	north	25, 50	no	open
Scenario 1.2	south	25, 50	no	open
Scenario 1.3	east	25, 50	no	open
Scenario 1.4	west	25, 50	no	open
Scenario 2.0	n/a	0	n/a	n/a
Scenario 3.0	n/a	0	yes	open
Scenario 3.1	north	25, 50	yes	open
Scenario 3.2	south	25, 50	yes	open
Scenario 3.3	east	25, 50	yes	open
Scenario 3.4	west	25, 50	yes	open
Scenario 4.0	n/a	0	n/a	n/a

4.0 HEAT FLUX FIRE MODEL INPUTS (SCENARIOS 1 & 3)

4.1 Design Fire Development

4.1.1 UL 9540A Summary

UL 9540A provides a test and data collection methodology for component level BESS equipment (cell, module, and unit level). UL9540A (4th edition) testing was performed on the Lithium Iron Phosphate (LFP) model LFP71173207 battery cells used in the Hithium BESS. A summary of the UL 9540A test data is provided in Appendix A for reference.

The UL 9540A data can be used to develop a representative design fire for a BESS container. It should be noted that the UL 9540A cell, module, and unit level tests showed cell venting without ignition and subsequent flaming of the vent gases. Although flaming was not observed to occur during the UL 9540A tests, a flaming failure may occur in the field due to varying conditions and therefore must be assumed for this analysis.

4.1.2 Design Fire Basis

A single worst-case design fire scenario was developed assuming a quasi-fully involved BESS container with its doors open. The model assumes the initiating BESS (i.e. location of design fire) is located on the lower-level because an initiating event on the lower level provides the greatest threat to vertically stacked BESS and structural members. Heat transfer is most severe in the vertical direction due to pre-heating from the flame front and direct flame impingement. Additionally, cooling of the lower structural members is difficult to achieve due to complex flow dynamics, water spray angles coverage, and blocking of water spray due to upper level BESS.

This design fire was applied to all model scenarios. The design fire is indicated as quasi-fully involved due to the propagation dynamics involving heating of a module before it becomes involved in a combustion event and burnout of the initiating modules over time, as all fuel is consumed in those modules. The container eventually reaches a steady-state condition where the number of propagating modules is approximately equal to the number of modules experiencing burnout.

The design fire scenario is conservative based on the UL 9540A tests which did not report flaming combustion in any of the reported tests (i.e. cell, module, or unit level). The initiating conditions and early fire development prior to reaching the quasi-steady state fire are not a limiting factor in this analysis (i.e. will not lead to worst case temperatures and heat fluxes) and are not included in the model. A variety of initiating factors could lead to the end result, that being a fully involved BESS fire. For example, an improperly mitigated deflagration during the early stages of thermal runaway could act as a catalyst for door failure and provide an ignition source for flaming combustion.

4.2 Design Fire Inputs

The gas mixture from the UL9540A cell level test was used to develop the representative chemical formula, soot yield, CO yield, and heat of combustion input to the FDS model. The UL9540A cell level data was normalized to remove contributions of CO₂ to ensure accurate calculation of the products of combustion. The chemical formula, soot yield, CO yield, and heat of combustion were calculated using a mass weighted average of individual constituents based

on the UL9540A gas composition, normalized without CO₂ contributions. The data for individual gas constituents was based on data provided in Appendix 3 of the SFPE Handbook. The gas mixture values used in the FDS model are shown in Table 2.

Table 2. Design fire FDS inputs

FDS parameter	Value
Chemical Formula	C _{0.28879} H _{1.34854} O _{0.16202}
CO Yield (g/g)	0.6153
Soot Yield (g/g)	0.0095
Heat of Combustion (kJ/kg)	25,904

The following methodology was used to calculate the steady state heat release rate for this model:

1. Calculate the total electrical energy stored inside of the Hithium BESS.
2. Convert the total electrical energy to a representative combustion energy.
3. Assume a conservative burning duration based on historical data, literature, and FRA's internal testing experience.
4. Divide the total combustion energy by the burning duration to determine the average BESS HRR².

The total electrical energy stored inside of the Hithium BESS is 5.016 MWh. The electrical energy is converted to a representative combustion energy using a conversion factor of 10 kJ/kJ resulting in a total combustion energy of 180.6 GJ [2]. Assuming a conservative burning duration of 3 hours for the BESS container, the calculated HRR is 16.7 MW. Three hours is considered a conservative burning duration because a longer burning duration will result in a lower average heat release rate and therefore lower incident heat flux and temperature conditions at target BESS and structural members. The calculated HRR is uniformly applied to the front surface area of each module in the BESS (venting location of each module).

4.3 CFD Model Geometry

4.3.1 Hithium BESS Geometry

The modelled BESS geometry was based on the Hithium BESS cabinet exterior setup and interior layout as shown in Figure 1. Each BESS unit is comprised of 6 racks of battery modules with each rack holding 8 battery modules and a PCS underneath each rack. Each BESS cabinet has a control enclosure at one end which contains ventilation and cooling equipment and a 920L containment system on the floor.

² Note, peak HRR's typically are 40-50% greater than the average HRR but are experienced for a short duration. For this reason, impacts of peak HRR are not included in this analysis.

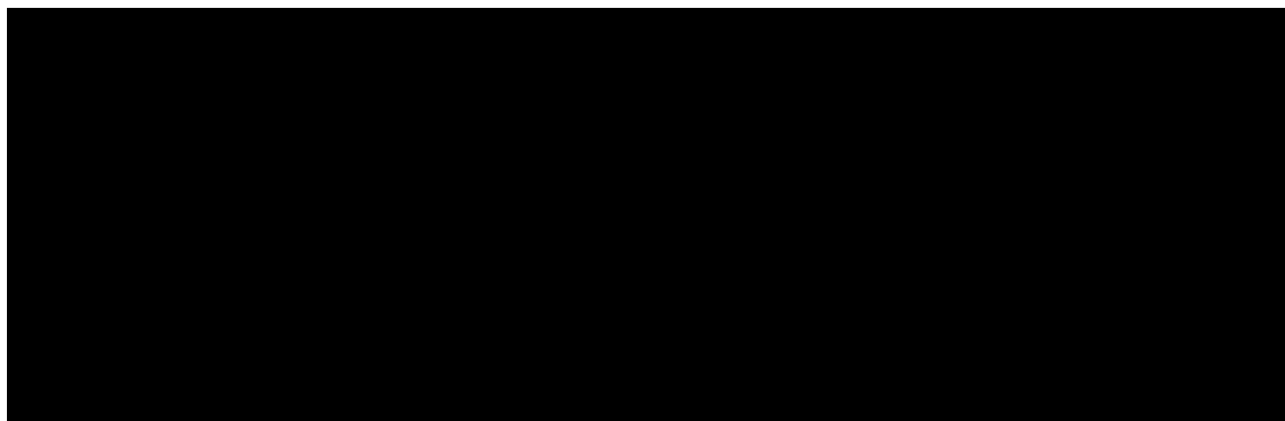


Figure 1. Hithium BESS container configuration; (a) exterior, (b) interior

The BESS container exterior dimensions are 19 ft 9 in (length) x 9 ft 5 in (height) x 7 ft 8 in (width) (6.058 m (length) x 2.896 m (height) x 2.4 m (width)). The ESS container exterior walls are modelled with a 2 mm steel exterior with a 50 mm wool board filled middle and a 3 mm steel plate interior. The module dimensions are modelled as 2.2 m (length) x 0.8 m (width) x 0.25 m (height), to align with the computation grid, with a 2 mm thick polypropylene top and 2.5 mm thick aluminum sides and bottom. All additional interior walls and components are assumed to be constructed of 5 mm thick steel. The following representative material properties were used in the model:

Table 3. FDS model material properties [1,7,8]

Material	Density (kg/m ³)	Conductivity (W/(m*K))	Specific heat (kJ/(kg*K))
Steel	7850	45.8	0.46
Wool Board Insulation	208	0.05 (20 °C) 0.1 (377 °C) 0.2 (677 °C)	0.8 (20 °C) 2.0 (677 °C)
Polypropylene	960	0.2	2.16
Aluminum	2707	204	0.896

The initiating unit was modelled with the cabinet doors open at a 90-degree angle from the BESS and all vent openings closed. The open-door scenario represents the worst-case potential fire scenario (due to the availability of oxygen) and subsequent heat flux to target containers. This is a common worst-case scenario evaluated in large-scale live fire testing and reflects the UL9540A unit level testing with an open rack. The modelled initiating unit is shown in Figure 2.

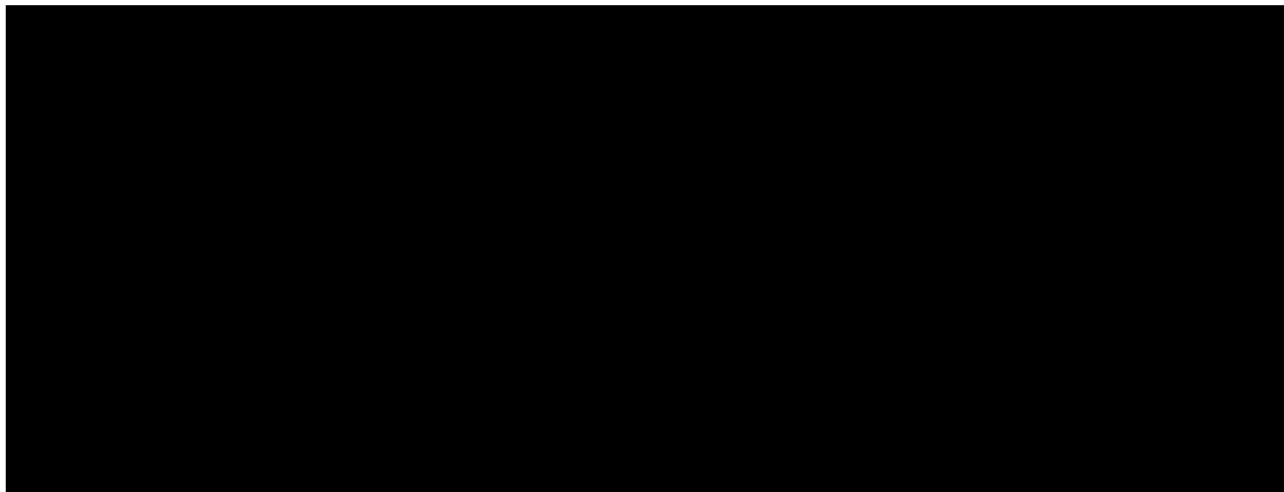


Figure 2. FDS model of Hithium BESS (front view of initiating unit)

4.3.2 Structural Geometry

The double stack arrangement and structural design were modelled based on the REVIT drawings developed by VHB received by FRA on July 9, 2024. A structural steel platform design is used to support the BESS arrangement. Representative structural steel members were included in the model to closely resemble the actual physical steel dimensions and to be resolved by the computational mesh.

The top level of BESS equipment is modelled as 15 ft (4.6 m) above the ground on metal grating. A clearance of approximately 5 ft (1.5 m) is provided from the top of the lower-level BESS to the platform metal grating. It is anticipated the future structural design will provide a greater clearance from the top of the lower-level BESS to the structure; however, the modelled clearance provides conservative results as greater clearances would result in a decrease in temperature and heat flux exposures. The proposed double stack arrangement is shown in Figure 3. On each level, the BESS are arranged to provide a minimum clearance of 1 ft (0.3m) side to side, 1 ft 9 inches (0.5 m) back-to-back, and 13 ft 11 in (4.2 m) in front.

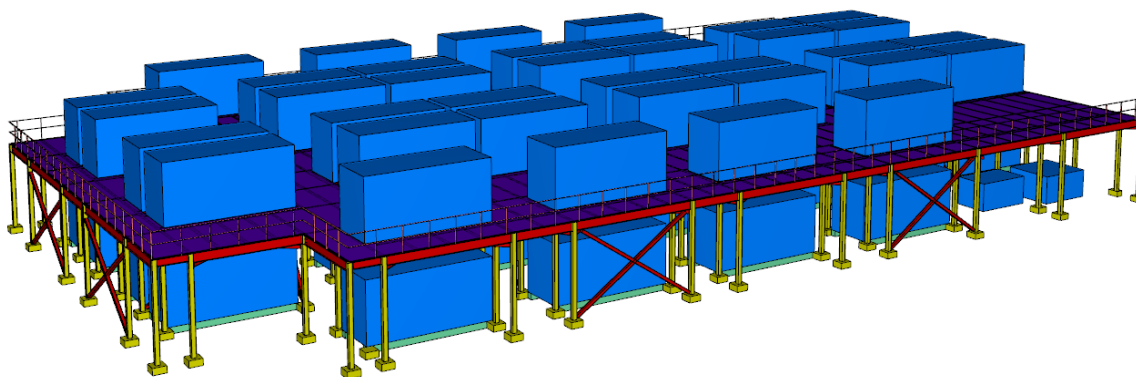


Figure 3. CAD drawing of Trimount Energy Storage double stack site arrangement

CFD Analysis

The CFD model includes a representative portion of the proposed site to reduce the size of the model domain and optimize run time while including appropriate wind and blocking effects. The metal grating supporting the upper level was modelled as a simplified structure with a representative open area on a 3.28 ft x 3.28 ft (1m x 1m) basis. The grating and structural supports were modeled as steel with the properties indicated in Table 3. The modelled double stack arrangement and structural design are shown in Figure 4.

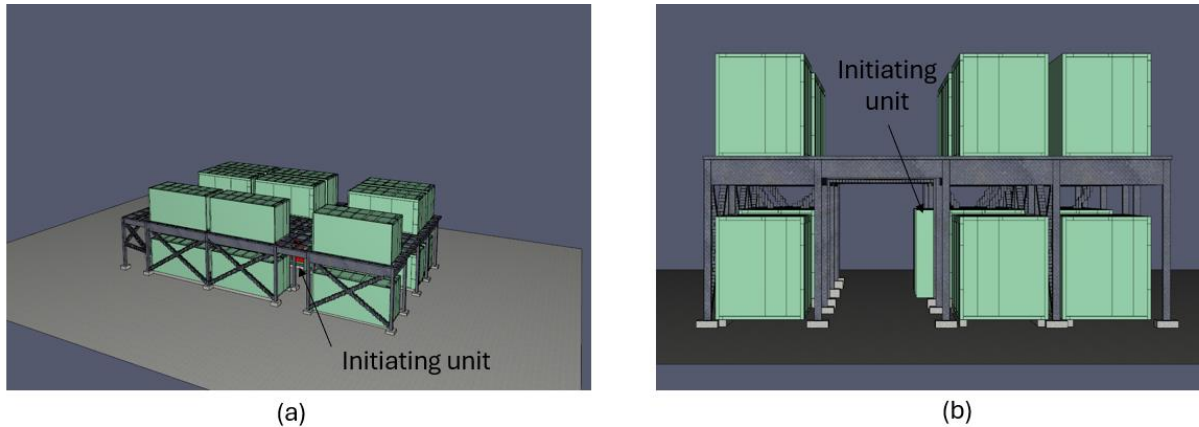


Figure 4. Trimount Energy Storage double stack model domain; (a) iso-view, (b) side view

4.4 External Fire Suppression Nozzle Model (scenario 3 only)

Representative water spray nozzles were utilized in the FDS model (scenario 3 only) to simulate the proposed minimum required design density across the exterior of the BESS units to evaluate cooling effects³. The nozzle locations and orientation were based on the fixed water spray design as shown in Figure 5 below. Additional details about the water spray design can be found in the Jupiter Power Everett Fire Protection BOD document developed by FRA. Small scale FDS simulations were developed to confirm that the target minimum design density is applied to the entire exterior of the BESS surface with the modelled nozzles.

³ The provided fixed water spray nozzle model is used to provide a proof-of-concept analysis. A future analysis should characterize the exact fixed water spray nozzles to be used in the design.

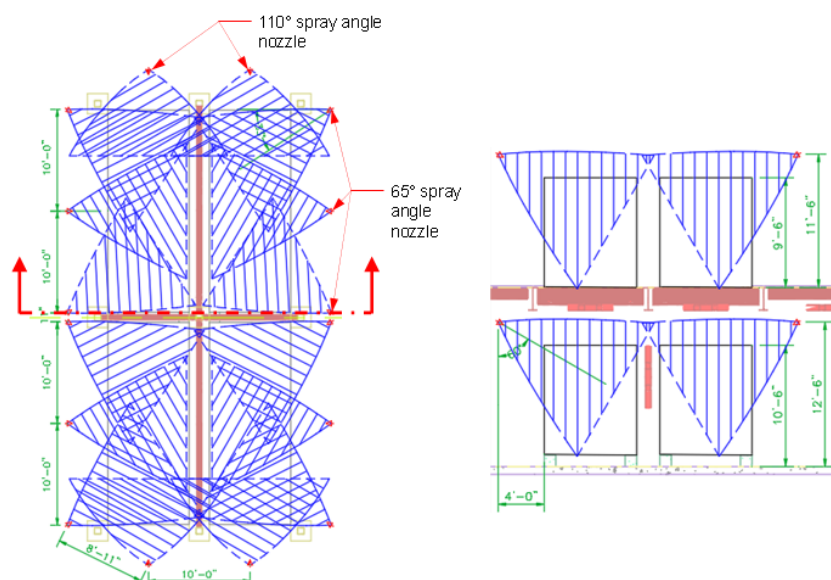


Figure 5. Plan (left) and section (right) view of water spray nozzle arrangement

The water spray nozzles were modelled with the following characteristics:

Table 4. FDS nozzle model inputs

FDS Parameter	Value
Flow rate (LPM)	116.11
Spray angle (degrees)	User specified spray pattern table ⁴
Particle Velocity (m/s)	15.11
Diameter (μm)	950
Gamma (-)	2.9
Particles per second (pps)	10,000

The water spray nozzles were assumed to be active for the entire simulation as the design fire assumes a full involved BESS. It is assumed the water spray nozzles would activate during the initial propagation stages and nozzles would be active by the time a BESS is fully involved. Water spray nozzles were initiated 10 seconds after the simulation initiation to allow the fire to stabilize prior to incorporating water spray effects.

4.5 Extinction Model

The extinction model in FDS was deactivated for this analysis. Therefore, it is conservatively assumed that the external fire suppression will have no impact on the fire development. Only surface cooling and radiative heat blocking effects were included in the external fire protection design analysis.

⁴ Spray pattern table is based on nozzle spray characterization in the patented 4S machine for the provided operating parameters in Table 4.

4.6 Grid Size

FDS uses a rectilinear mesh to discretize the computational domain. A computational mesh of 0.1 m x 0.1 m x 0.1 m was implemented in the vicinity of the initiating and target BESS to resolve the fire dynamics and was increased to 0.2 m x 0.2 m x 0.2 m a minimum of one BESS length away from the initiating unit. The grid size was further increased outside of the domain of primary interest (structural supports and BESS unit area) to 0.4 m x 0.4 m x 0.4 m to allow for/incorporate wind and boundary effects.

The FDS user manual provides guidelines to determine the underlying grid size [3-6]. It defines a non-dimensional parameter of the plume resolution index, D^*/dx , where dx is the nominal size of a cell and D^* is the characteristic fire diameter. This is used as a guide to determine an appropriate cell size. D^* is defined in the equation below:

$$D^* = \left(\frac{\dot{Q}}{\rho_{\infty} C_p T_{\infty} \sqrt{g}} \right)^{2/5} \quad (\text{eq. 1})$$

Where:

\dot{Q} is the heat release rate in kW

T_{∞} is the ambient air temperature in K

C_p is the specific heat of air in kJ/kg.K

g is the acceleration due to gravity (m/sec²)

ρ_{∞} is the atmospheric air density (kg/m³)

The ratio of D^*/dx indicates how many grid cells span a fire with an ideal diameter of D^* . According to the FDS validation guide, FDS has been validated for values of D^*/dx between 8 and 20 for similar models. For the chosen grid resolution in the current analysis, the D^*/dx is 29 and 14 in the 0.1m area and 0.2m resolution area respectively. The provided grid resolution exceeds the existing FDS verification range in the fine grid area and is within the verified range in the medium grid resolution area. Higher plume resolution index values indicate more resolved fire dynamics.

4.7 Ambient Conditions

The ambient conditions utilized in each model are summarized in Table 5.

Table 5. FDS scenario 1 & 3 model ambient conditions

FDS Parameter	Input Value
Temperature (°C)	25
Relative Humidity (%)	50
Wind Directions	North, South, East, & West

CFD Analysis

Wind Speeds (MPH) ¹	25 & 50
--------------------------------	---------

Notes 1: A ramp up time of 10 seconds was included between wind speeds to prevent numerical instabilities.

4.8 Simulation Duration

Each simulation completed 60 seconds of simulation time at steady state conditions plus the time required for wind and water spray initialization (approximately 10-20 seconds depending on the wind direction).

5.0 1D HEAT TRANSFER MODEL INPUTS (SCENARIOS 2 & 4)

5.1 BESS Geometry

The BESS geometry used in the 1D heat transfer model was identical to the BESS geometry indicated in Section 4.3.1. The model domain is limited to a single target BESS (i.e. non-initiating unit). The model domain is shown in Figure 6 for reference.

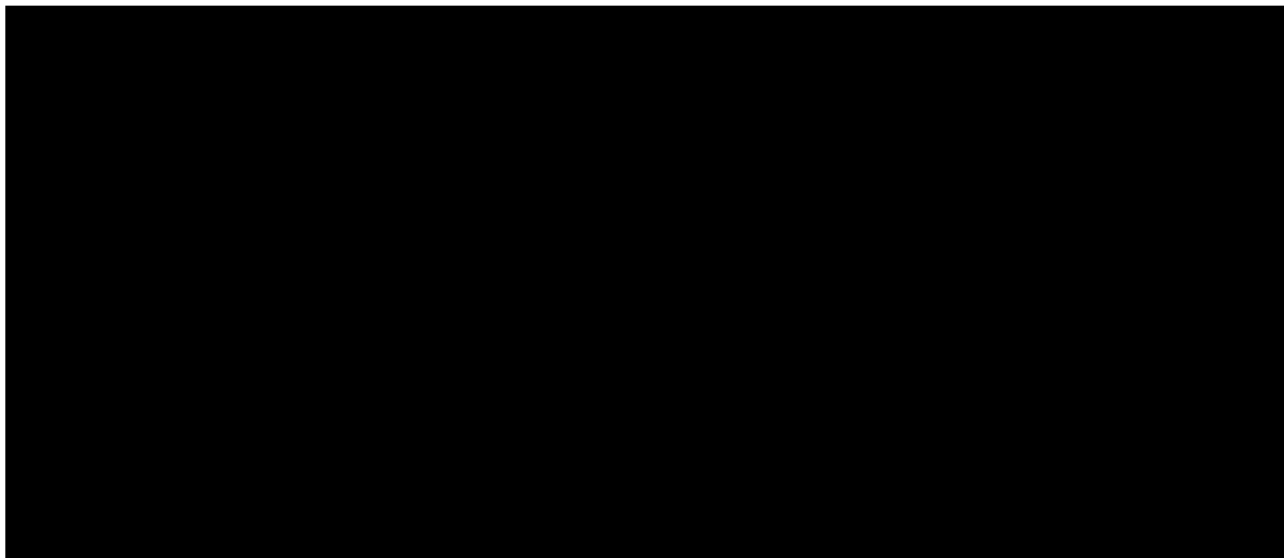


Figure 6. 1D heat transfer FDS model domain (a) entire domain, (b) single rack model resolution

5.2 Boundary Conditions

The 1D heat transfer models do not directly model the fire source or nozzle effects as was done for Scenarios 1 & 3. Rather, the results of Scenarios 1 & 3 for external heat fluxes experienced at the target BESS unit (with and without fixed water spray system) are applied as constant heat fluxes to the representative exterior wall surface areas of the target BESS. These fixed heat flux values are based on the worst-case instantaneous conditions determined through the heat flux fire model analysis.

The external heat flux is applied to the outside of the BESS front and bottom surfaces. The heat flux is conservatively applied with a minimum of three ranges (high heat flux, medium heat flux, and low heat flux) where the upper bound of the range is applied to the entire affected surface area within that range. The applied heat fluxes for scenario 2 (no fixed water spray) and 4 (with fixed water spray) are shown in Figure 7 and Figure 8 respectively. Note, these heat flux values are based on the worst-case results of the heat flux models as provided in Section 6.0 of this report.

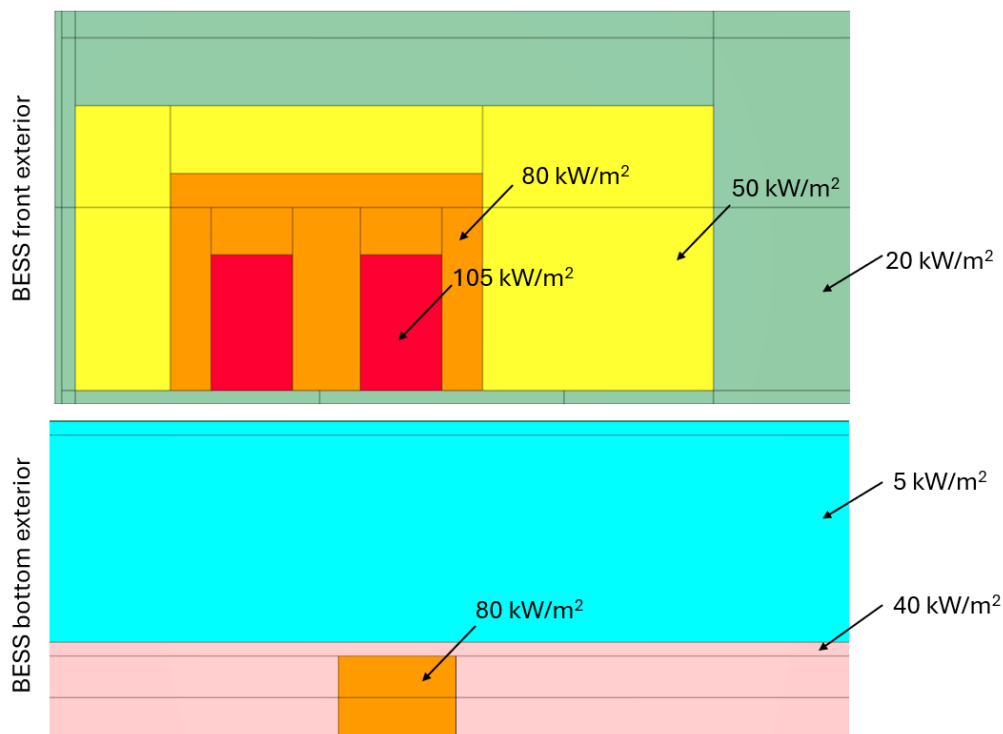


Figure 7. Scenario 2 applied external heat flux (1D heat transfer without external water spray)

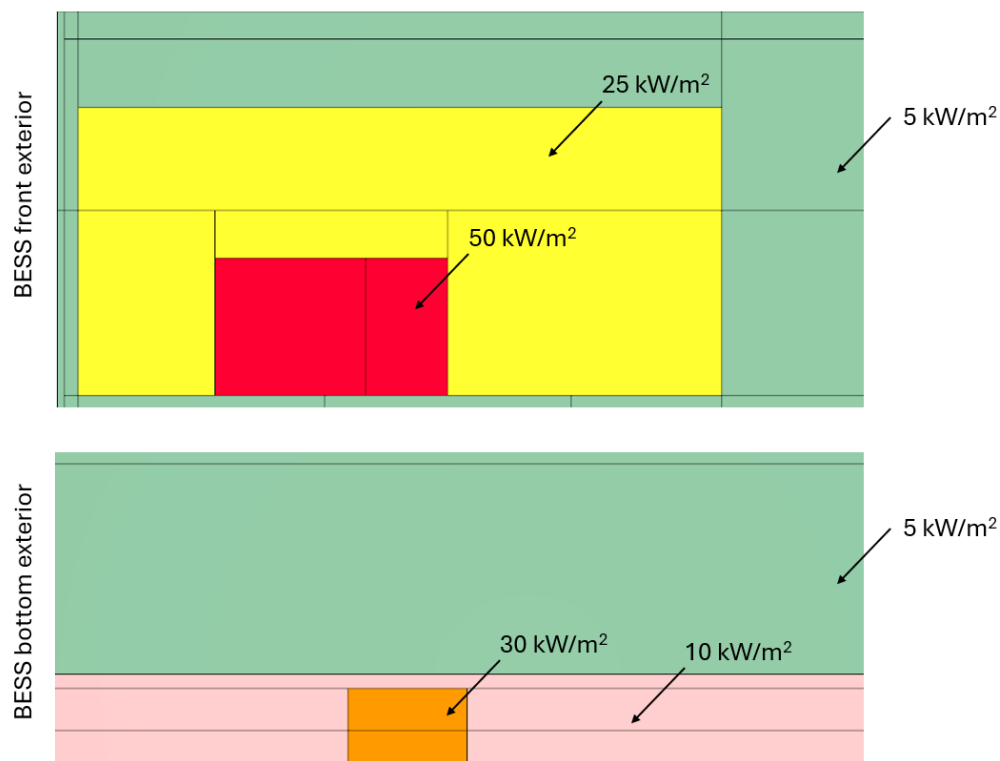


Figure 8. Scenario 4 external applied heat flux (1D heat transfer with external water spray)

5.3 Other Model Inputs

The grid size, ambient conditions, and simulation duration utilized in each 1D heat flux model are summarized in Table 6.

Table 6. FDS scenario 2 & 4 model ambient conditions

FDS Parameter	Input Value
Grid Size ¹ (m)	0.05
Temperature (°C)	25
Relative Humidity (%)	50
Simulation Duration ² (seconds)	3,600

Notes 1: A ramp up time of 10 seconds was included between wind speeds to prevent numerical instabilities.
2: Simulates a long duration exposure and allows the interior module temperatures to reach equilibrium based on the applied external heat flux.

6.0 FDS MODEL RESULTS & ANALYSIS

The following sections report the results of the FDS models. Results provided in the main body of this report include only those for the worst-case heat flux exposure conditions and the associated 1D heat flux results. Results for all additional scenarios are provided in Appendix C.

Five (5) types of figures are provided for each scenario variation in which the following output quantities are provided:

1. A three-dimensional representation of the fire and smoke produced by the fire including water droplet visualization where applicable.
2. Integrated heat flux at 12 kW/m², which represents an approximate boundary for some class A combustible materials to be potentially ignited by the thermal radiation exposure.
3. Integrated heat flux at 30 kW/m², which represents an approximate boundary for damage to exposed electrical equipment at the thermal radiation exposure.
4. Incident heat flux (kW/m²) exposure to surfaces in the domain used to visualize the location of the peak exposure.
5. Adiabatic surface temperature (°C) which is a measure of the net heat transfer to the surface, including incident exposures and cooling effects and is a useful input metric for heat transfer analysis.

The below figures show representative instantaneous values for the simulation duration, with representative summary results tables provided to compile the duration of exposure and approximate affected surface areas for representative heat flux ranges. Results summaries show significant fluctuations in incident heat flux and surface temperature values over time due to the flame structure and water-cooling effects (for models with active suppression).

The results presented in this section follow the naming convention and view orientations as shown in Figure 9.

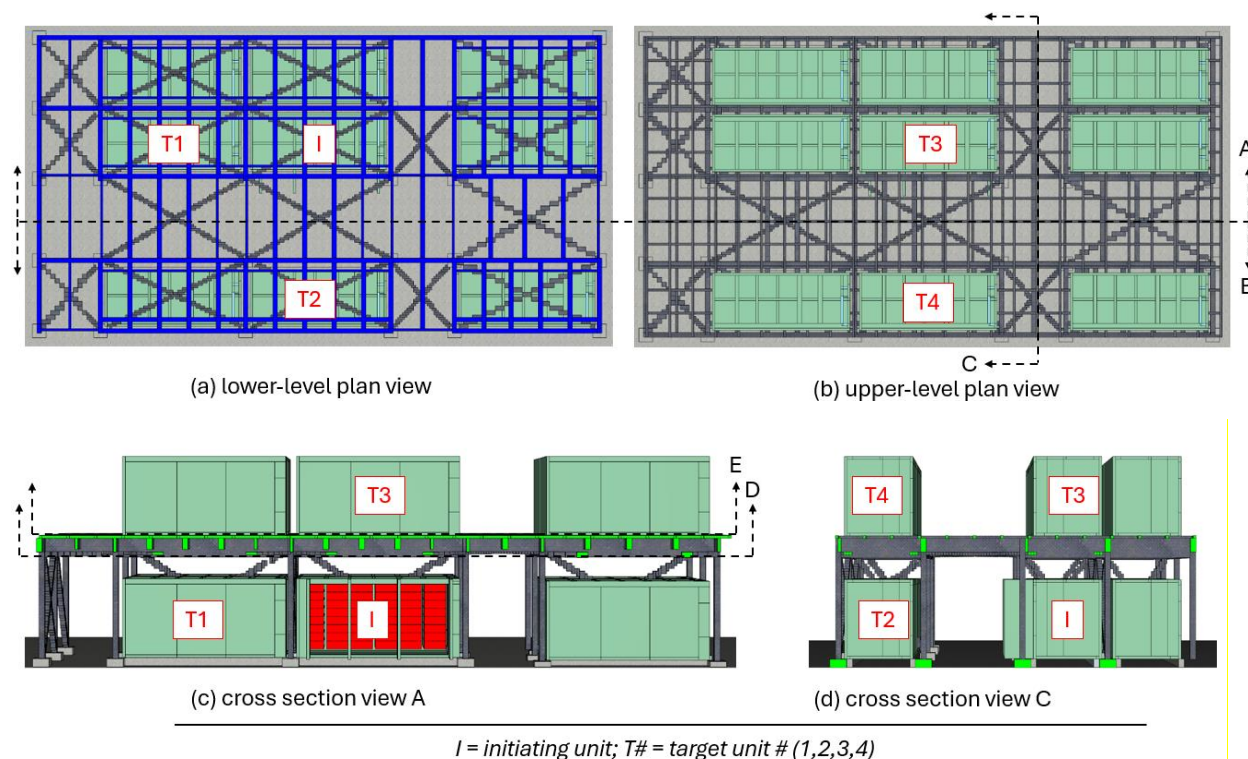


Figure 9. FDS results nomenclature guide

6.1 Scenario 1.0 Results (0 wind)

Scenario 1 evaluates external heat flux conditions to target BESS units and structural members without any external fire protection. After reviewing the results, it was determined the most severe exposure conditions occurred with no wind, to target unit 3 (T3) located directly above the initiating unit (I). Figure 10 shows an isometric view of the initiating BESS heat and smoke visualization.



Figure 10. 3D Smokeview visualization of smoke and heat

CFD Analysis

Figure 11 shows a 3D contour of the boundary of 12 kW/m^2 and 30 kW/m^2 areas respectively. Figure 12 shows the incident heat flux experienced on BESS and structural surfaces respectively. The results images show incident heat flux values between 0 kW/m^2 (blue) and 32.5 kW/m^2 (red).

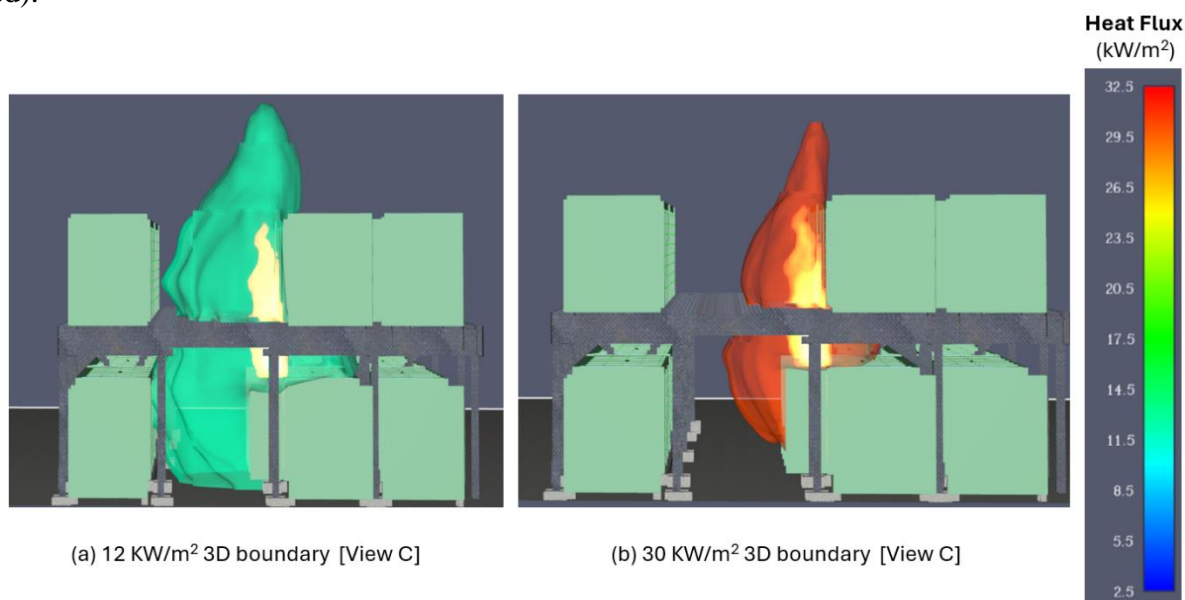


Figure 11. Integrated heat flux (a) at 12 kW/m^2 ; (b) 30 kW/m^2 [view C]

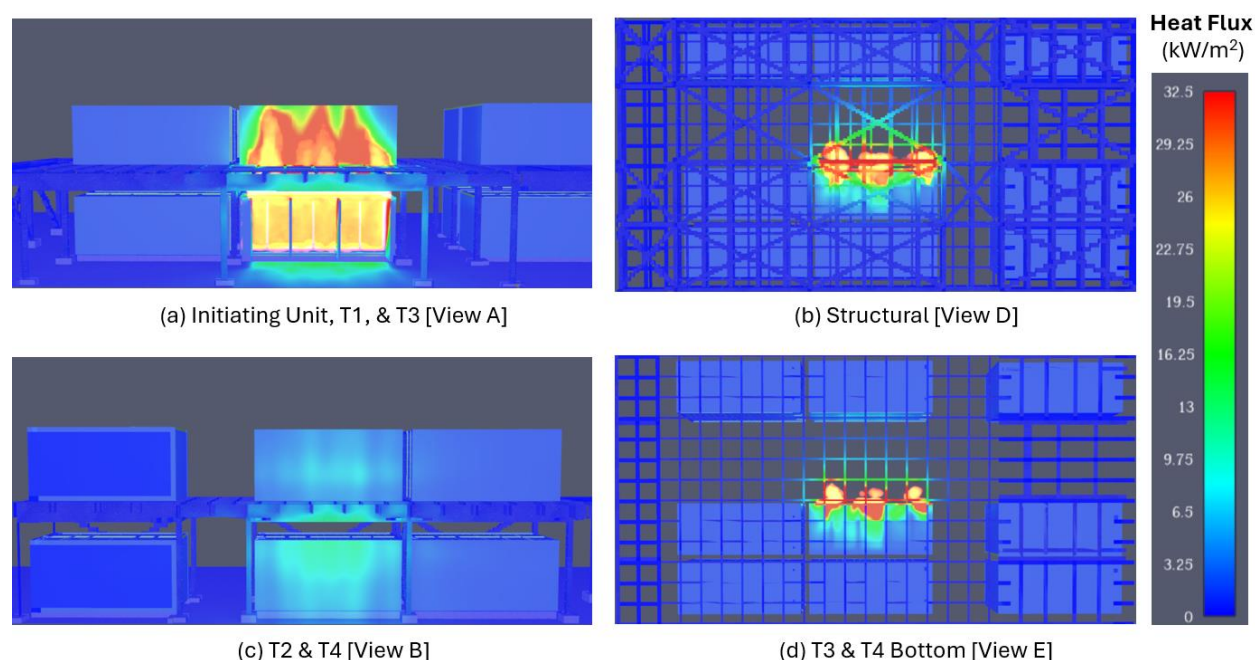


Figure 12. Incident heat flux at (a) View A, (b) View D, (c) View B, (d) View E

Figure 13 shows the adiabatic surface temperature of BESS and structural steel members. The results images show surface temperature values between 25°C (blue) and 538°C (red).

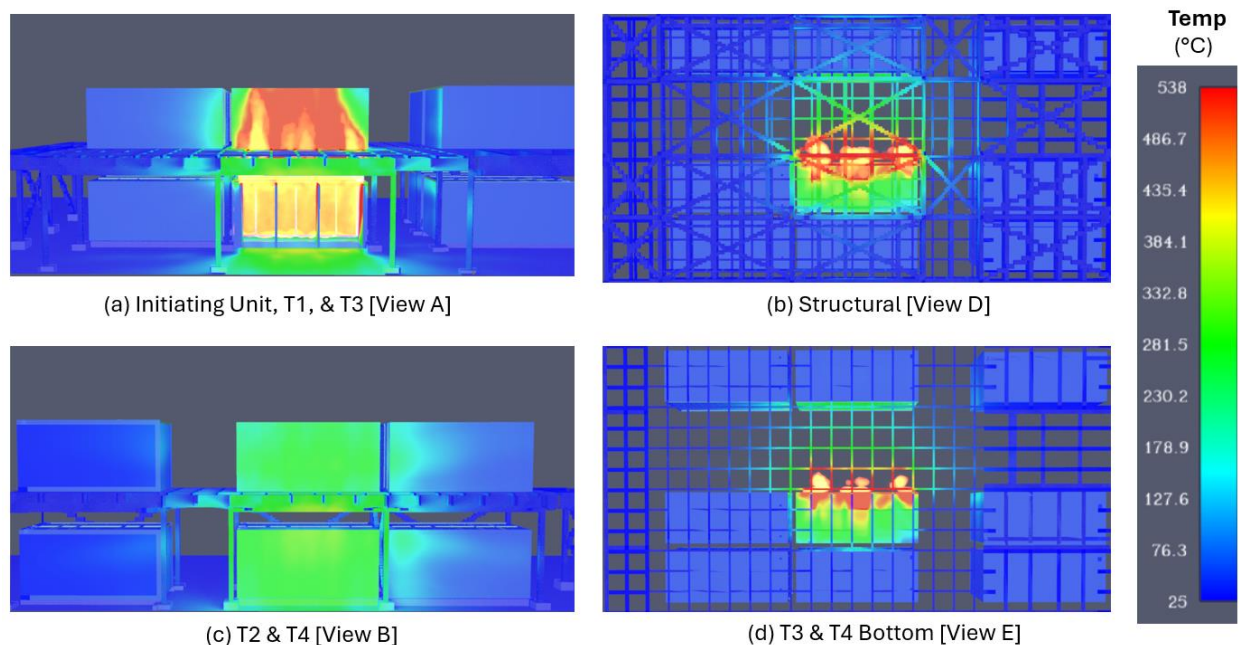


Figure 13. Surface temperature at (a) View A, (b) View D, (c) View B, (d) View E

The results show that the front and bottom surface of T3 and localized structural members above the initiating BESS are exposed to high incident heat fluxes and temperatures. T3 and representative structural members are consistently exposed to heat fluxes and temperatures of 70 kW/m^2 and 700°C respectively. T3 and representative structural members are exposed to peak values of 140 kW/m^2 and 974°C respectively for short durations.

6.1.1 T3 time dependent heat flux analysis

In addition to the 2D and 3D result visualizations provided above, ninety-six (96) heat flux devices were provided equally spaced along the front surface of target BESS. The results show that T3 experienced the highest incident heat flux. The T3 heat flux device outputs were analyzed to quantify the affected surface area and associated time duration to provide a more wholistic view of the results. Heat flux device outputs are provided approximately every 15 seconds. Table 7 utilizes representative heat flux ranges based on the maximum incident heat flux to show the impact to the BESS front surface area with time.

Table 7. Scenario 1: time dependent heat flux analysis

Heat Flux Range¹ (kW/m²)	Percentage affected surface area² (%)	Approximate affected surface area³ (m²)	Percentage of simulation duration⁴ (%)
2-35	97.9	17	61.65
35-70	80.2	13.9	31.02
70-100	45.8	7.9	6.76
100-140	16.6	2.9	0.57

Notes 1: Four approximately equal ranges were developed based on the maximum instantaneous heat flux measured in the model.

2: The percentage affected area is estimated by assuming each thermocouple represents an equal portion of the BESS front surface area. The total number of thermocouples whose measurements are within a representative heat flux range are summed and divided by the total number of thermocouples. This estimate includes all surface areas that are affected throughout the entire simulation without accounting for the associated time duration.

3: Estimated by multiplying the percentage of affected surface area by the front surface area of the BESS (17.4 m²)

4: The percentage of simulation duration is estimated by first summing the total number of time steps for each unique device within the indicated heat flux range divided by the total number of timesteps (233). This value is then summed across all devices for the given heat flux range and normalized by the total number of devices (96). The percentage of simulation duration indicates the percentage of the simulation duration in which heat flux values are in the indicated range.

The analysis shows that the majority of the front exterior surface of the BESS is exposed to heat fluxes between 2-35 kW/m² and 35-70 kW/m² with heat fluxes being in the lower range approximately 60% of the simulation duration and in the higher range for approximately 30% of the simulation duration. The front surface experiences peak heat fluxes up to 100 kW/m² and 140 kW/m² for short durations (~6% and 0.5% respectively). The primary scenario results provided in Section 6.2 correspond to the typical heat flux values experienced ~93% of the time at the exterior surface and the secondary scenario results correspond to the peak flux values experienced ~ 7% of the time at the exterior surface.

6.1.2 Structural members time dependent temperature analysis

A simplified analysis was conducted to evaluate the duration and peak temperature exposure to the structural steel members.

North American standard ASTM E119 specifies a critical endpoint temperature criterion of 704°C (1300°F), for a single point temperature, for loaded steel roof beams [9]. For the purpose of this analysis ASTM E119 structural steel critical temperatures are used to provide a comparison to the FDS results. Note, ASTM E119 is used to evaluate fire resistance rating of structural members and is provided for reference only, a specific analysis relating to the load bearing strength of the structural members utilized in this design should be completed and is outside the scope of this analysis. A detailed image of the results of the temperature impacts to the structural steel is provided in Figure 14.

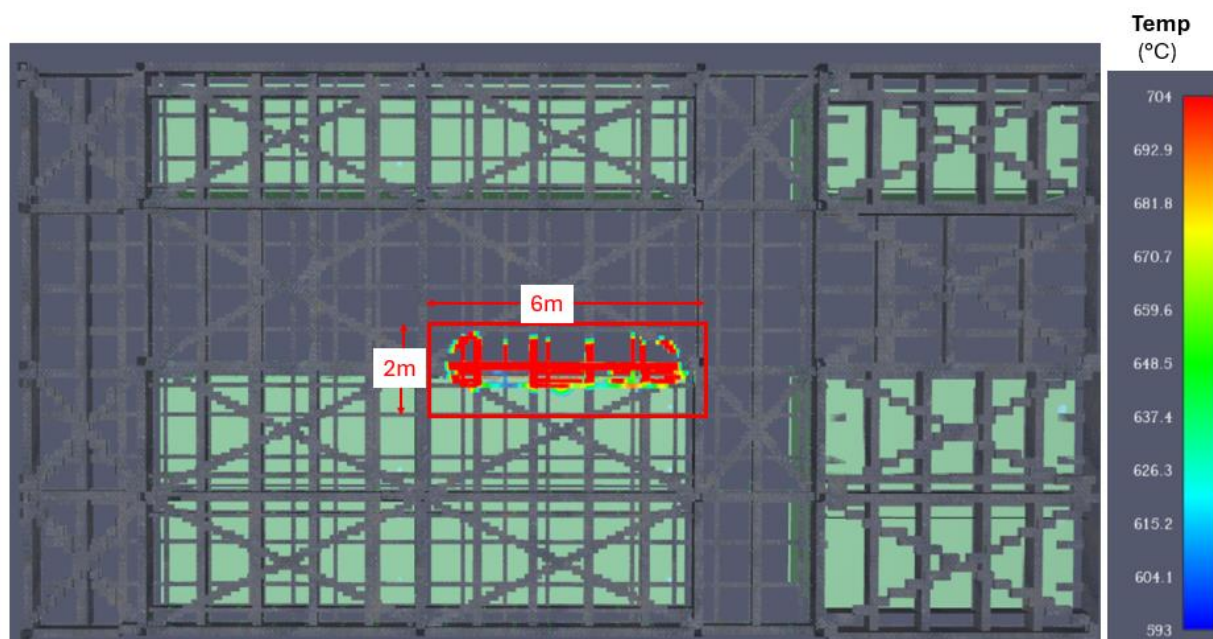


Figure 14. Structural steel temperature results visualization

The results show that the area of steel subject to temperatures greater than 704 °C (representative instantaneous failure temperature of steel) is approximately 6m x 2m in an area directly above the initiating BESS unit. Instantaneous peaks reach up to 1050 °C for short durations over an area less than 1m². The peak temperature values, durations, and impacted areas are summarized in Table 8.

Table 8. Time dependent structure temperature results summary

	Value
Average temperature exposure (°C)	>704
Duration	Constant/ continuous
Impacted area (m²)	12
Peak instantaneous temperature (°C)	1050
Duration (seconds)	< 1
Impacted area (m²)	~1

6.2 Scenario 2.0 Results (0 wind)

Scenario 2 applies the typical worst-case external heat flux boundary conditions from scenario 1 to a small scale 1D heat flux model to calculate the internal BESS module level surface temperature for target BESS. The worst-case external heat flux conditions were observed at T3 for the no wind conditions.

Thermocouple devices were placed on the front of each of the target modules to measure the surface temperature in the model. The output of the thermocouple devices over time are provided in Figure 15.

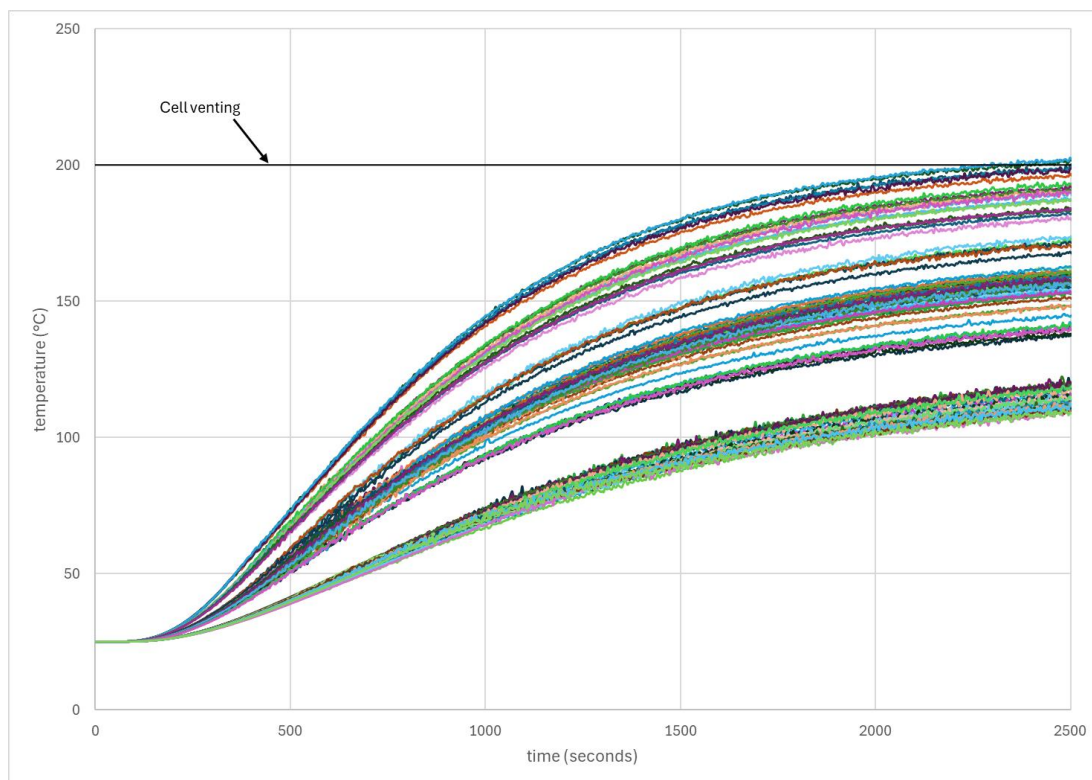


Figure 15. Scenario 2 internal target module surface temperature

The results show that module temperatures exceed the cell venting temperature within 2500 seconds. Additionally, the module temperatures have not yet reached steady state and are expected to further exceed the cell venting temperature over a longer exposure duration.

It should be noted that the results of this analysis are valid for the modelled scenario; however, real life conditions may deviate from the modelled inputs. For this reason, a second heat flux model was completed using a single external heat flux applied to the entire exterior assuming long duration exposure to peak heat fluxes (corresponds to ~7% exposure duration in Table 7). A peak heat flux of 105 kW/m^2 and 80 kW/m^2 was applied to the exterior front and bottom surface of the BESS respectively. The results of this simulation are provided as a worse case analysis and provide bounding results. The temperatures of interior modules are provided in Figure 16.

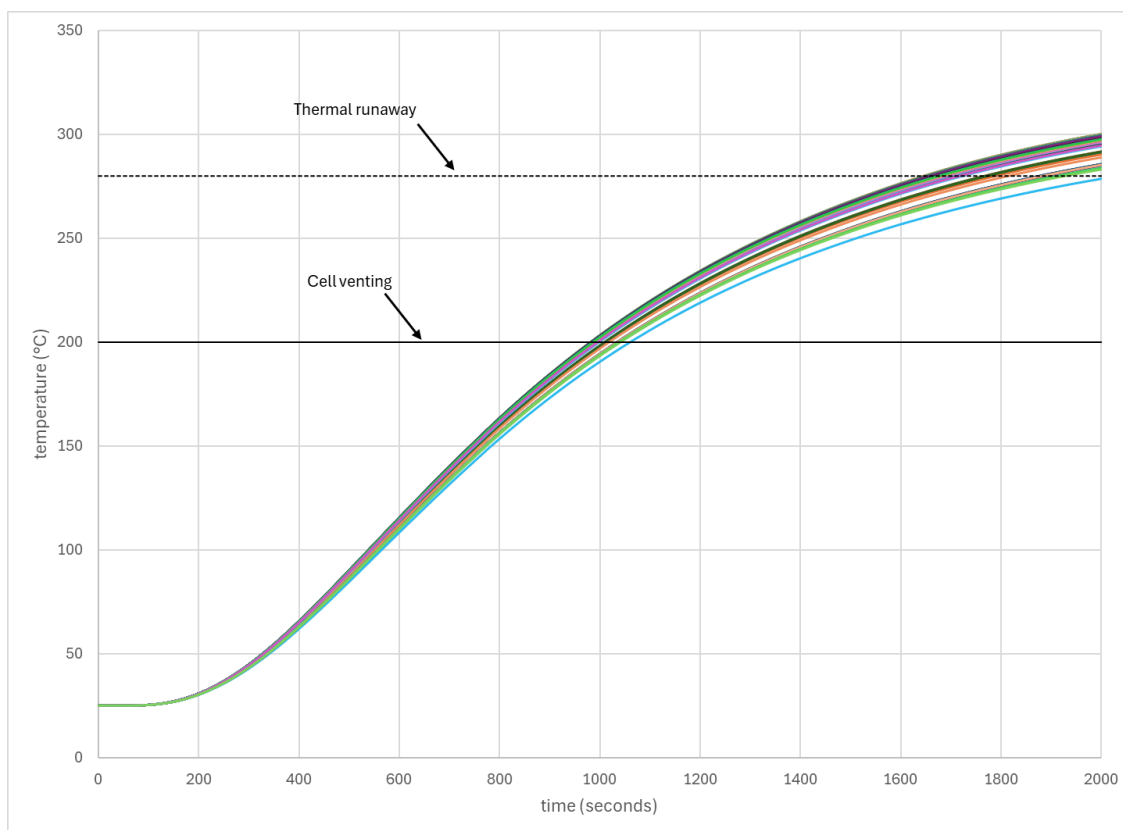


Figure 16. worst case target module surface temperature

The results of this analysis show that both the module surface temperature exceeds both the cell venting and thermal runaway temperature within 2000 seconds and are continually increasing with time.

6.3 Scenario 3.0 Results (0 wind)

Scenario 3 evaluates external heat flux conditions to target BESS units and structural members including the effects from the external water spray system. After reviewing all of the results, it was determined the most severe exposure conditions occurred with no wind to target 3 (T3) located directly above the initiating unit (I). Figure 17 shows an isometric view of the initiating BESS heat and smoke visualization and nozzle water droplets.

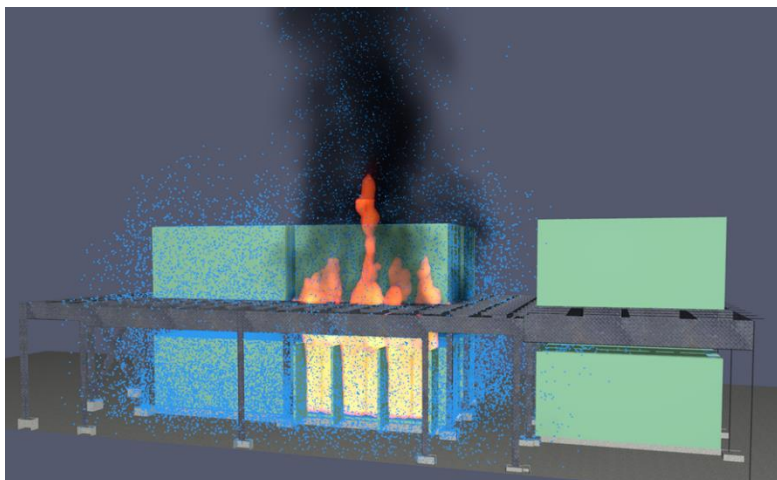


Figure 17. 3D Smokeview visualization of smoke and heat

Figure 18 shows a 3D contour of the boundary of 12 kW/m² and 30 kW/m² areas respectively. Figure 19 shows the incident heat flux experienced on BESS and structural surfaces respectively. The results images show incident heat flux values between 0 kW/m² (blue) and 32.5 kW/m² (red).

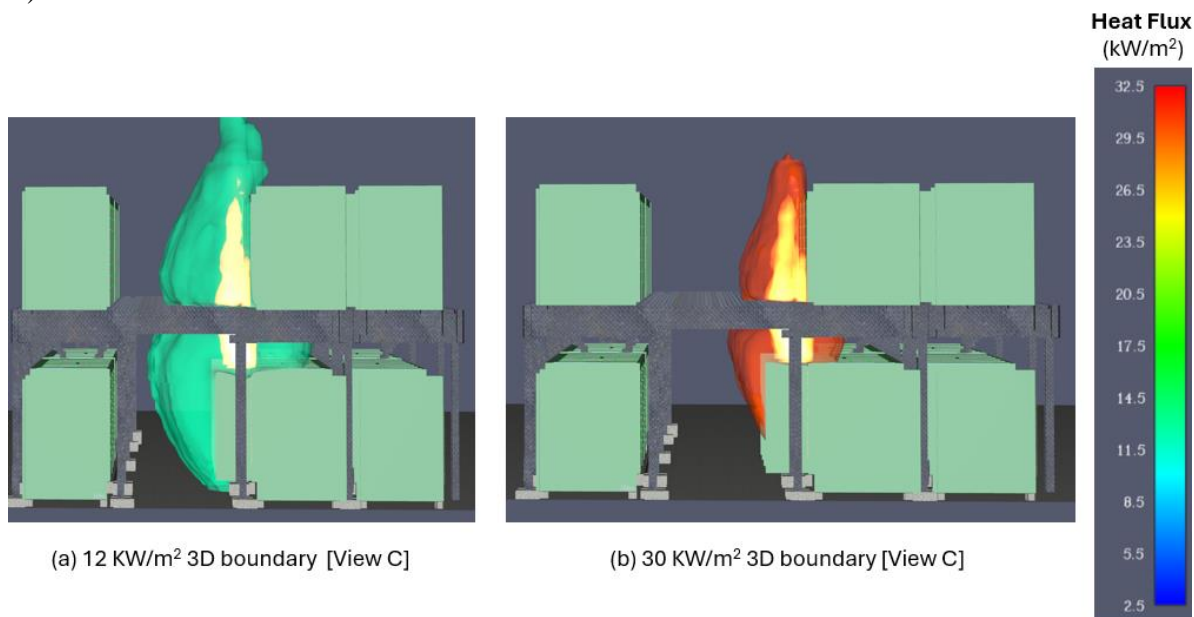


Figure 18. Integrated heat flux (a) at 12 kW/m²; (b) 30 kW/m² [view C]

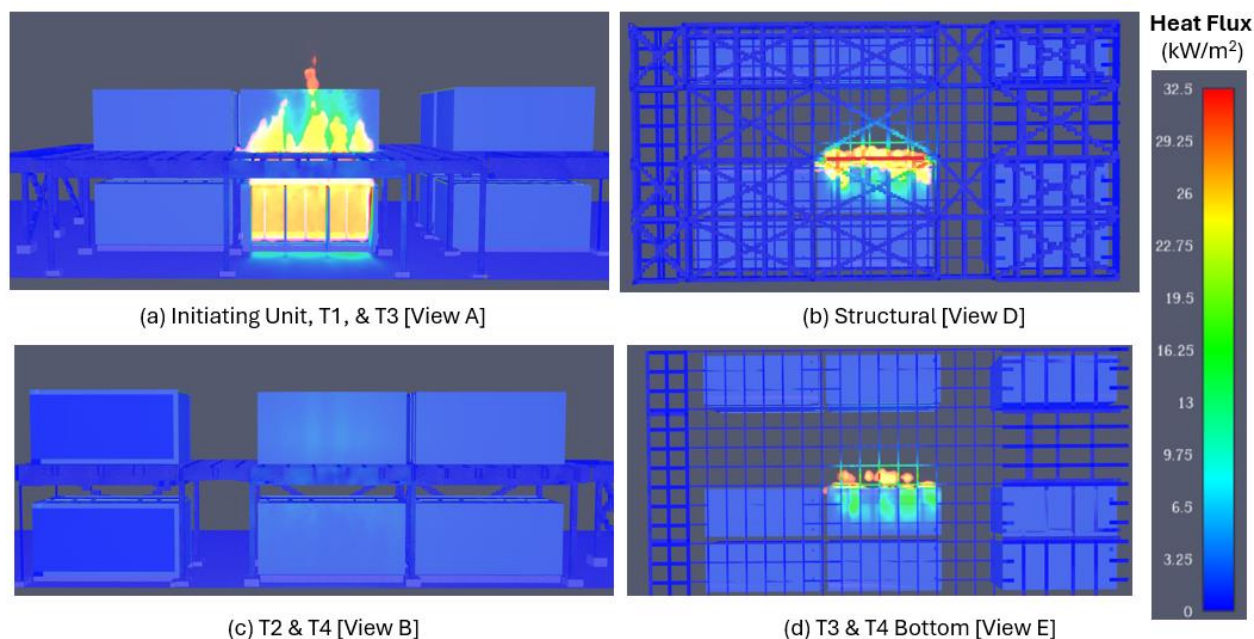


Figure 19. Incident heat flux at (a) View A, (b) View D, (c) View B, (d) View E

Figure 20 shows the adiabatic surface temperature of BESS and structural steel members. The results images show surface temperature values between 25 °C (blue) and 538 °C (red).

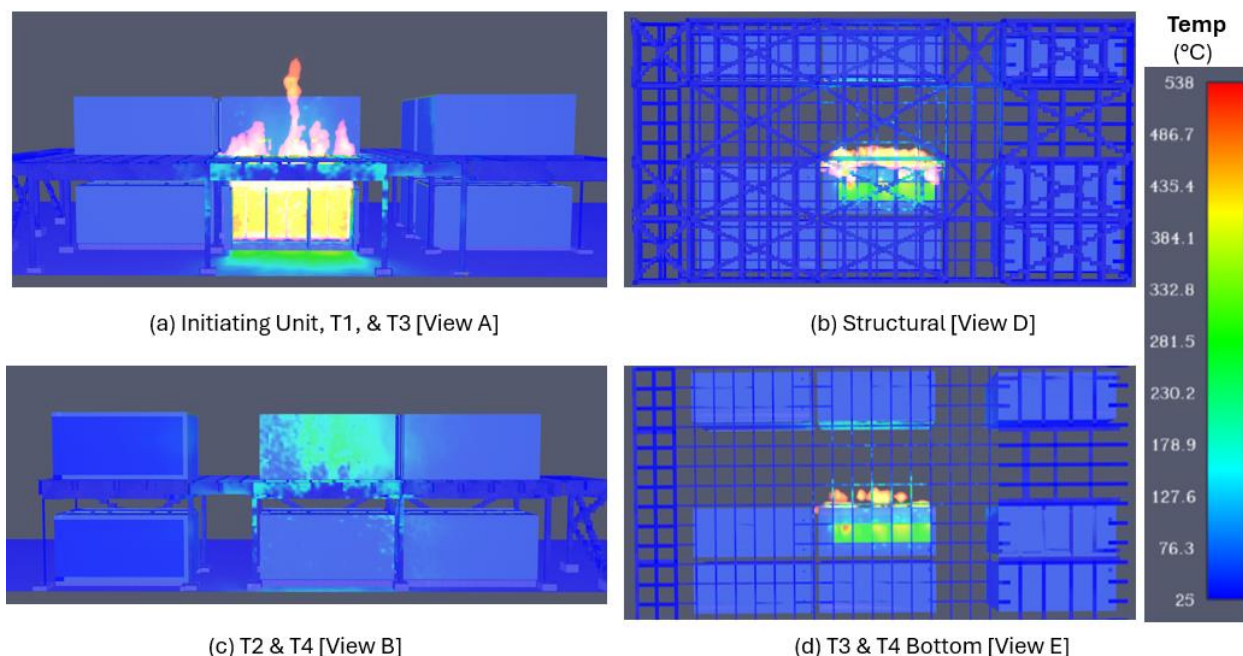


Figure 20. Surface temperature at (a) View A, (b) View D, (c) View B, (d) View E

The results show that incident heat flux and surface temperatures experienced at the front and bottom surface of T3 and localized structural members above the initiating BESS are significantly reduced compared to Simulation 1. T3 and representative structural members are consistently exposed to heat fluxes and temperatures of 30 kW/m² and 150 °C respectively. T3

and representative structural members are exposed to peak values of 55 kW/m² and 584 °C respectively for short durations.

6.3.1 T3 time dependent heat flux analysis

In addition to the 2D and 3D result visualizations provided above, ninety-six (96) heat flux devices were provided equally spaced along the front surface of target BESS. The results show that T3 experienced the highest incident heat flux. The T3 heat flux device outputs were analyzed to quantify the affected surface area and associated time duration to provide a more wholistic view of the results. Heat flux device outputs are provided approximately every 15 seconds. Table 9 utilizes representative heat flux ranges based on the maximum incident heat flux to show impact to the BESS front surface area with time.

Table 9. Scenario 3: time dependent heat flux analysis

Heat Flux Range ¹ (kW/m ²)	Percentage affected surface area ² (%)	Approximate affected surface area ³ (m ²)	Percentage of simulation duration ⁴ (%)
0-15	91.6%	15.95	58.15%
15-30	81.25%	14.2	39.65%
30-45	46.8%	8.1	2.16%
45-55	5.3%	0.92	0.03%

Notes 1: Four approximately equal ranges were developed based on the maximum instantaneous heat flux measured in the model.
2: The percentage affected area is estimated by assuming each thermocouple represents an equal portion of the BESS front surface area. The total number of thermocouples whose measurements are within a representative heat flux range are summed and divided by the total number of thermocouples. This estimate includes all surface areas that are affected throughout the entire simulation without accounting for the associated time duration.
3: Estimated by multiplying the percentage of affected surface area by the front surface area of the BESS (17.4 m²)
4: The percentage of simulation duration is estimate by first summing the total number of time steps for each unique device within the indicated heat flux range divided by the total number of timesteps (233). This value is then summed across all devices for the given heat flux range and normalized by the total number of devices (96). The percentage of simulation duration indicates the percentage of the simulation duration in which heat flux values are in the indicated range.

The analysis shows that the majority of the front exterior surface of the BESS is exposed to heat fluxes between 0-15 kW/m² and 15-30 kW/m² with heat fluxes being in the lower range approximately 60% of the simulation duration and in the higher range for approximately 40% of the simulation duration. The front surface experiences peak heat fluxes up to 45 kW/m² and 55 kW/m² for short durations (~2% and 0.03% respectively). Note, the peak heat flux ranges and durations are significantly reduced from Scenario 1.

6.3.2 Structural members time dependent temperature analysis

A simplified analysis was conducted to evaluate the duration and peak temperature exposure to the structural steel members.

North American standard ASTM E119 specifies a critical endpoint temperature criterion of 593°C (1100°F), for the average section temperature, for loaded steel roof beams [9]. For the purpose of this analysis ASTM E119 structural steel critical temperatures are used to provide a comparison to the FDS results. Note, ASTM E119 is used to evaluate fire resistance rating of structural members and is provided for reference only, a specific analysis relating to the load bearing strength of the structural members utilized in this design should be completed and is outside the scope of this analysis. A detailed image of the results of the temperature impacts to the structural steel is provided in Figure 25.

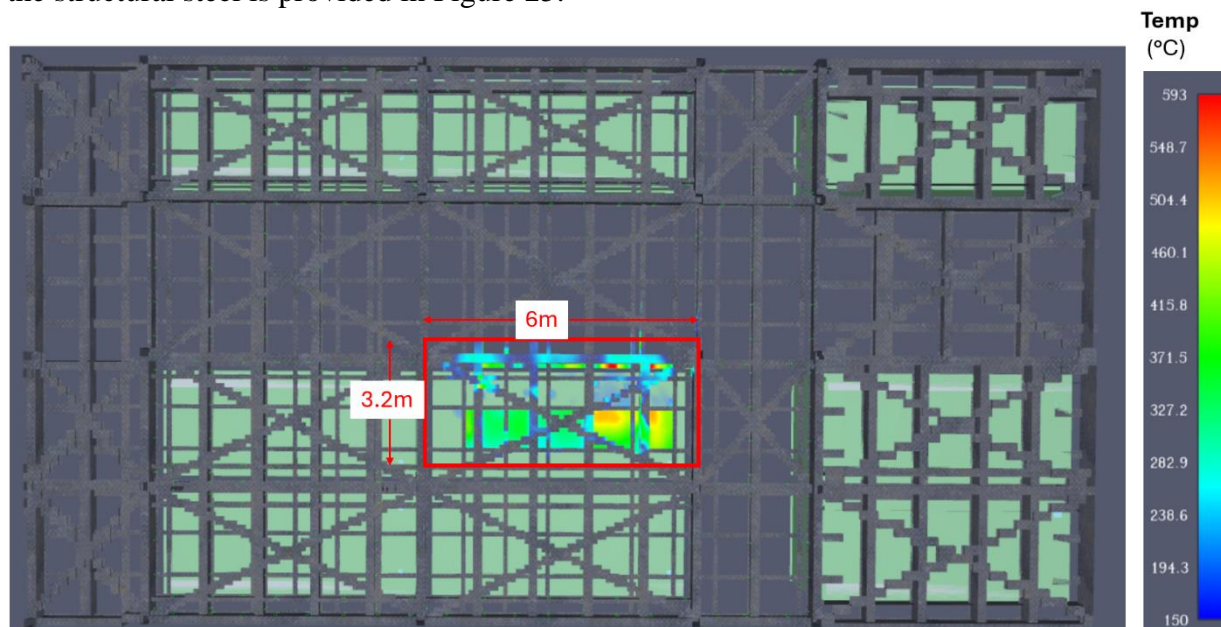


Figure 21. Structural steel temperature results visualization

The results show that overall temperature impact to the structural steel is significantly reduced with the addition of the water spray system. The average maximum temperature experienced at the structure is 150 °C (shown in blue) which impacts an area approximately equal to the footprint of the BESS (19.2 m²). Instantaneous peaks are maintained below 598 °C which for the purposes of this analysis is considered the long duration temperature exposure threshold for steel. The peak temperature values, durations, and impacted areas are summarized in Table 10.

Table 10. Time dependent structure temperature results summary

	Value
Average temperature exposure (°C)	150
Duration	Constant/ continuous
Impacted area (m²)	19.2
Peak instantaneous temperature (°C)	<598
Duration (seconds)	< 1
Impacted area (m²)	~0.5

6.4 Scenario 4.0 (0 wind)

Scenario 4 applies the worst-case external heat flux boundary conditions from scenario 3 to a small scale 1D heat flux model to calculate the internal BESS module level surface temperature

for target BESS. The worst-case external heat flux conditions were observed at T3 for the no wind conditions.

Thermocouple devices were placed on the front of each of the modules to measure the surface temperature in the model. The output of the thermocouple devices over time are provided in Figure 22.

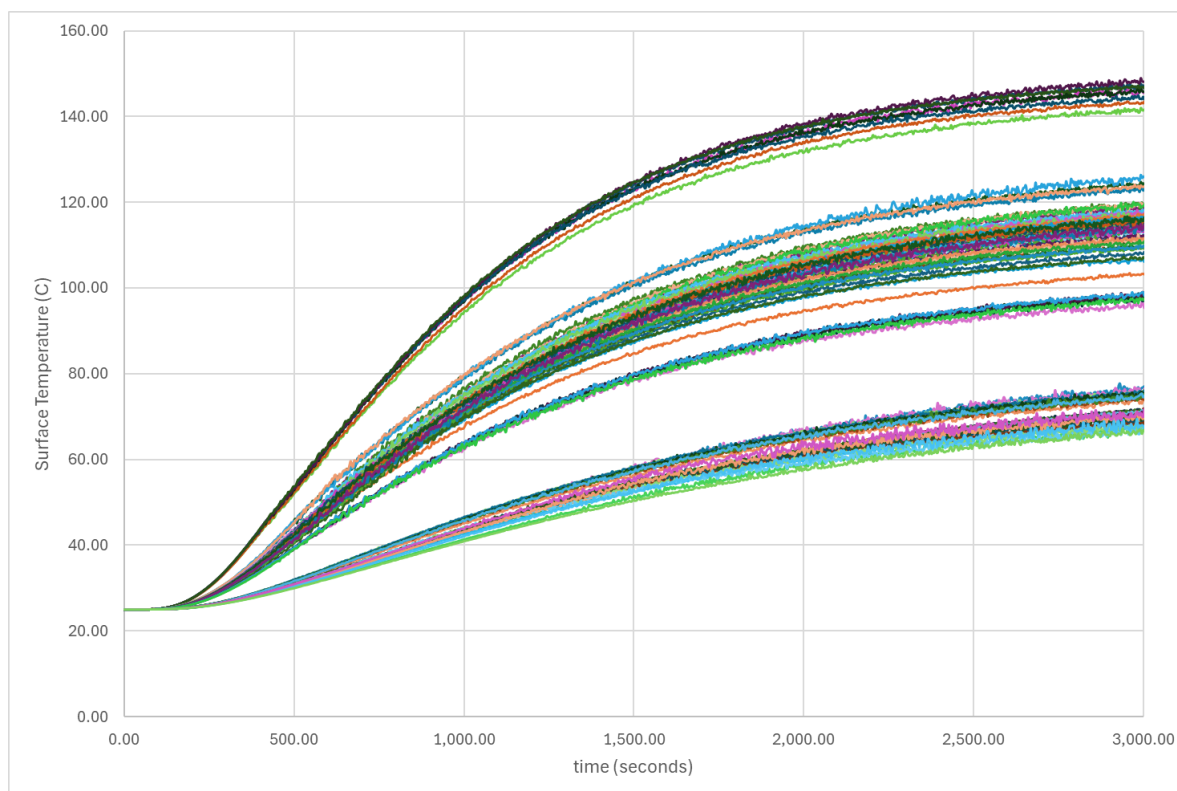


Figure 22. Module surface temperature

The results show that for a long duration exposure (1 hour), the external fixed water spray system is able to reduce the temperature experienced at the module level compared to the results without any external fire protection. The module temperature approaches a steady state temperature less than 160 °C, this provides a 25% safety factor below the minimum cell venting temperature and a 75% safety factor below the minimum thermal runaway temperature. Based on these results, thermal runaway propagation to adjacent containers is highly unlikely to occur with external fire protection for the modelled scenarios and configuration.

6.5 Results and Analysis Summary

Two scenarios were evaluated, one without any exterior fire protection and one with an exterior fixed water spray system. The results without the water spray system show target BESS and structural members are consistently exposed to heat fluxes and temperatures in excess of 70 kW/m² and 700°C, respectively, with peak values up to 100% greater. The simulations modeling the impact of the proposed external water spray system showed over a 50% reduction in peak external heat fluxes and temperatures on the exterior of target BESS.

Table 11 provides a comparative analysis of time duration and intensity of external heat flux to the front surface of T3 with and without the fixed water spray system. The comparative analysis shows that the external spray system significantly decreases the average maximum and peak instantaneous heat flux values and decreases both the surface area and duration of peak heat fluxes compared to the results without the external spray system (scenario 1).

Table 11. Comparative time dependent heat flux analysis for T3 exterior

Heat Flux Range ¹ (kW/m ²)	Percentage affected surface area ² (%)		Approximate affected surface area ³ (m ²)		Percentage of simulation duration ⁴ (%)	
	w/o water spray	w/ water spray	w/o water spray	w/ water spray	w/o water spray	w/ water spray
2-35	97.9	100	17	17.4	61.65	99.54%
35-70	80.2	25	13.9	4.25	31.02	0.46%
70-100	45.8	0.0	7.9	0.0	6.76	0.0%
100-140	16.6	0.0	2.9	0.0	0.57	0.0%

Notes

- 1: The four heat flux ranges from Scenario 1 were utilized to provide a comparative analysis between simulations with and without active external fire protection.
- 2: The percentage affected area is estimated by assuming each thermocouple represents an equal portion of the BESS front surface area. The total number of thermocouples whose measurements are within a representative heat flux range are summed and divided by the total number of thermocouples. This estimate includes all surface areas that are affected throughout the entire simulation without accounting for the associated time duration.
- 3: Estimated by multiplying the percentage of affected surface area by the front surface area of the BESS (17.4 m²)
- 4: The percentage of simulation duration is estimate by first summing the total number of time steps for each unique device within the indicated heat flux range divided by the total number of timesteps (233). This value is then summed across all devices for the given heat flux range and normalized by the total number of devices (96). The percentage of simulation duration indicates the percentage of the simulation duration in which heat flux values are in the indicated range.

The results also showed that without the water spray system the structural members are consistently exposed to average peak temperatures in excess of 704°C (1300°F), which is identified as the instantaneous failure criteria in ASTM E119, and peak instantaneous temperatures up to 1100 °C. The results with the water spray system decrease the average peak temperature to less than 150 °C and the peak instantaneous temperature to less than 593 °C. Figure 23 provides a side-by-side comparison of the Smokeview temperature visualization with (Scenario 1) and without (Scenario 3) the external water spray system. The results are plotted between 150 °C (blue) and 793 °C (red), areas subject to temperatures less than 150 °C are removed from the results visualization.

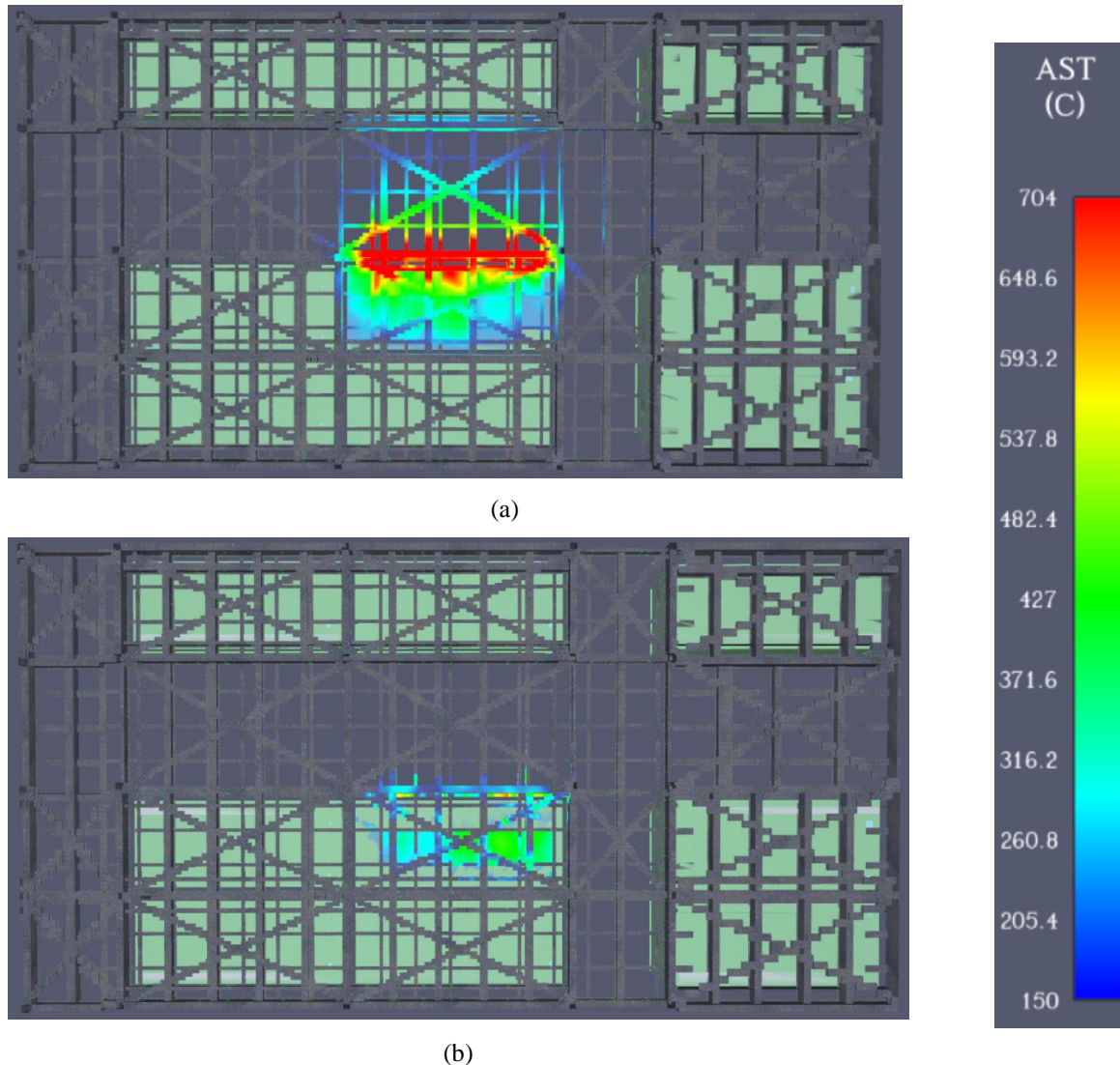


Figure 23. (a) Scenario 1 (b) scenario 3 structural temperature results comparison

The 1D models found that without external fire protection, modules within target BESS located above the initiating unit exceed the cell venting temperature for the modelled conditions (primary model). The results also showed that with bounding exterior heat flux conditions (secondary model), modules in target BESS exceeded both the cell venting and thermal runaway temperatures. With the addition of the exterior water spray system, heat transfer to the modules within target BESS was significantly reduced. Modules reached a steady state temperature of less than 160 °C, which provides a 25% safety factor to the critical cell venting temperature and a 75% safety factor to the cell thermal runaway temperature based on the UL 9540A cell level test data. Figure 24 plots the highest module temperature curve for each modeled condition for reference. Without any exterior fire protection, thermal runaway propagation is possible due to a fully involved fire event occurring on the lower level. Thermal runaway propagation can be prevented with the addition of the external water spray system.

CFD Analysis

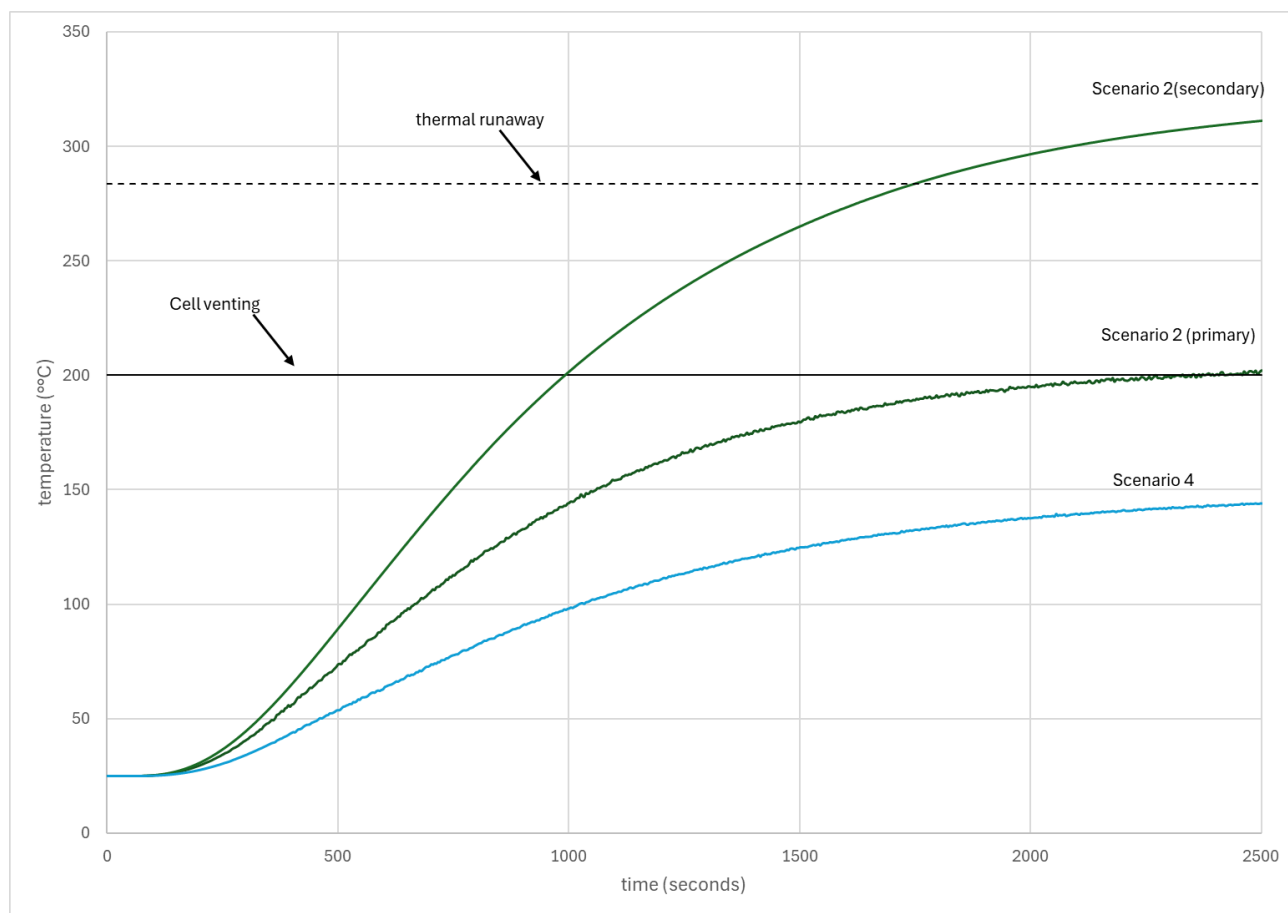


Figure 24. Module surface temperature comparison

7.0 CONCLUSION

The FDS modeling analysis was completed to evaluate the thermal consequences (heat flux & temperature) associated with a fully involved Lithium BESS fire event for the Trimount Energy Storage project. FDS simulations were completed to evaluate the external applied heat flux to target BESS and associated internal module surface temperature, as well as surface temperatures of structural members of the steel platform structure supporting the upper-level BESS equipment.

Based on the analysis presented herein, an external water spray system is required to prevent thermal runaway propagation between BESS units for a fully involved BESS fire on the lower level. Additionally, the water spray system is able to significantly reduce both the duration and intensity of the incident heat flux and temperature experienced at the steel structure. The current analysis shows that this is a feasible solution as it has provided capable cooling to the structure as well as preventing fire propagation to containers above and adjacent. Further structural analysis will confirm the feasibility of this design as it progresses.

All observations, conclusions, and recommendations are relevant only to this project and for the conditions, parameters, and assumptions described herein.

8.0 REFERENCES

- [1] Drysdale, D. (2011) An Introduction to Fire Dynamics. Wiley. DOI: 10.1002/9781119975465
- [2] Mayonado, J. et al. (2024) Advancing Li-Ion BESS Safety: *Comprehensive Testing and Meta-Analysis for Optimized Hazard Mitigation* [whitepaper].
- [3] McGrattan, K., et al.(a) National Institute of Standards and Technology. Fire Dynamics Simulator: Users Guide. Sixth Edition, May 28, 2021.
- [4] McGrattan, K., et al.(b) National Institute of Standards and Technology. Fire Dynamics Simulator Technical Reference Guide Volume 1: Mathematical Model. Sixth Edition, June 28,2022.
- [5] McGrattan, K., et al.(c) National Institute of Standards and Technology. Fire Dynamics Simulator Technical Reference Guide Volume 2: Verification. Sixth Edition, June 28,2022.
- [6] McGrattan, K., et al.(d) National Institute of Standards and Technology. Fire Dynamics Simulator Technical Reference Guide Volume 3: Validation. Sixth Edition, June 28,2022.
- [7] Quintiere, J. (2016) Principles of Fire Behavior. Second edition.
<https://doi.org/10.1201/9781315369655>
- [8] SFPE, “Appendix 3: Fuel Properties Combustion Data,” in SFPE Handbook of Fire Protection Engineering, Fifth Edition, 2016
- [9] “ASTM E119-16a: Standard Test Methods for Fire Tests of Building Construction and Materials.” 2016.

A. REFERENCE DRAWINGS

The following drawings were utilized in development of this analysis:

Document Name	Date
UL 9540A cell level test report #CN23F118 001	12/06/2023
UL 9540A module level test report #CN23XXY9 003	05/11/2024
UL 9540A unit level test report #CN244DBX 001	04/26/2024
Jupiter Power – Structural	07/15/24
Hithium_3D Model_ESS Container_5015kWh_Enclsoure Drawing	01/06/2024
Hithium Gen 2 general arrangement 1.01	08/10/2023
Hithium_DW_ESS Container_5015kWh_Electrical Drawings (UL)	10/11/2023
Hithium_DW_ESS Container_5015kWh_Mechanical Drawings (UL)	01/25/2024
Hithium_TI_Two ESS Containers Stacking Application-Mechanical Analysis	03/01/2024
Hithium_TI_ESS Container_5015kWh_Fire Protection system(UL)	11/16/2023

B. UL 9540A TEST REPORT SUMMARY

UL9540A testing was performed on the Lithium Iron Phosphate (LFP) model LFP71173207 battery cells used in the Hithium BESS. The cell vent gas composition is provided in Table 12 and the cell failure temperatures are provided in Table 13. The cell level test report indicated that approximately 101 L of battery vent gas was produced when the cell underwent thermal runaway. The minimum recorded temperatures indicating cell venting and thermal runaway were 200.7 °C and 283.5 °C respectively based on the cell level tests.

Table 12. Constituent concentrations based on cell level test data

Gas component	Concentration (v, %)
CH ₄	3.671
C ₂ H ₆	0.548
C ₂ H ₄	1.389
C ₃ H ₈	0.18
C ₃ H ₆	0.745
n-C ₄ H ₁₀	0.068
n-C ₄ H ₈	0.22
n-C ₅ H ₁₂	0.076
iso-C ₅ H ₁₂	0.112
n-C ₅ H ₁₀	0.053
CO	16.202
CO ₂	26.861
H ₂	49.875

Table 13. Cell failure temperatures

Ambient conditions at the initiation of the test.....:	26.1°C, 51%R.H.	27.9°C, 51%R.H.	26.1°C, 52%R.H.	27.9°C, 50%R.H.	26.1°C, 51%R.H.
Sample number	#1 ¹⁾	#2	#3	#4	#5
Open circuit voltage before test (V) :	3.35	3.37	3.36	3.35	3.35
Cell vent temperature (°C)	231.4	201.8	200.7	208.5	203.6
Thermal runaway onset temperature (°C)	328.8	306.3	283.5	291.4	301.6
Average cell vent temperature (°C) ²⁾	--	203.7			
Average thermal runaway onset temperature (°C) ²⁾	--	295.7			
Note:					
1) The sample (#1) is for gas vent capture.					
2) The temperatures were averaged over the tested samples (#1, #2, #3, #4, #5) excluding the gas vent capture sample (#1).					

In addition to cell testing, UL9540A (4th edition) module level testing (LM010401-A) and unit level testing (LC083502) were also completed. The heater location and preparation for the module level test is shown in Figure 25. The results of the module level test indicated that one cell was forced into thermal runaway via external heating and one cell entered thermal runaway through cell-to-cell propagation. It should be noted that the results appear to indicate three cells went into thermal runaway but only two cells are indicated in the report. No flaming or flying debris were observed during the module level test.

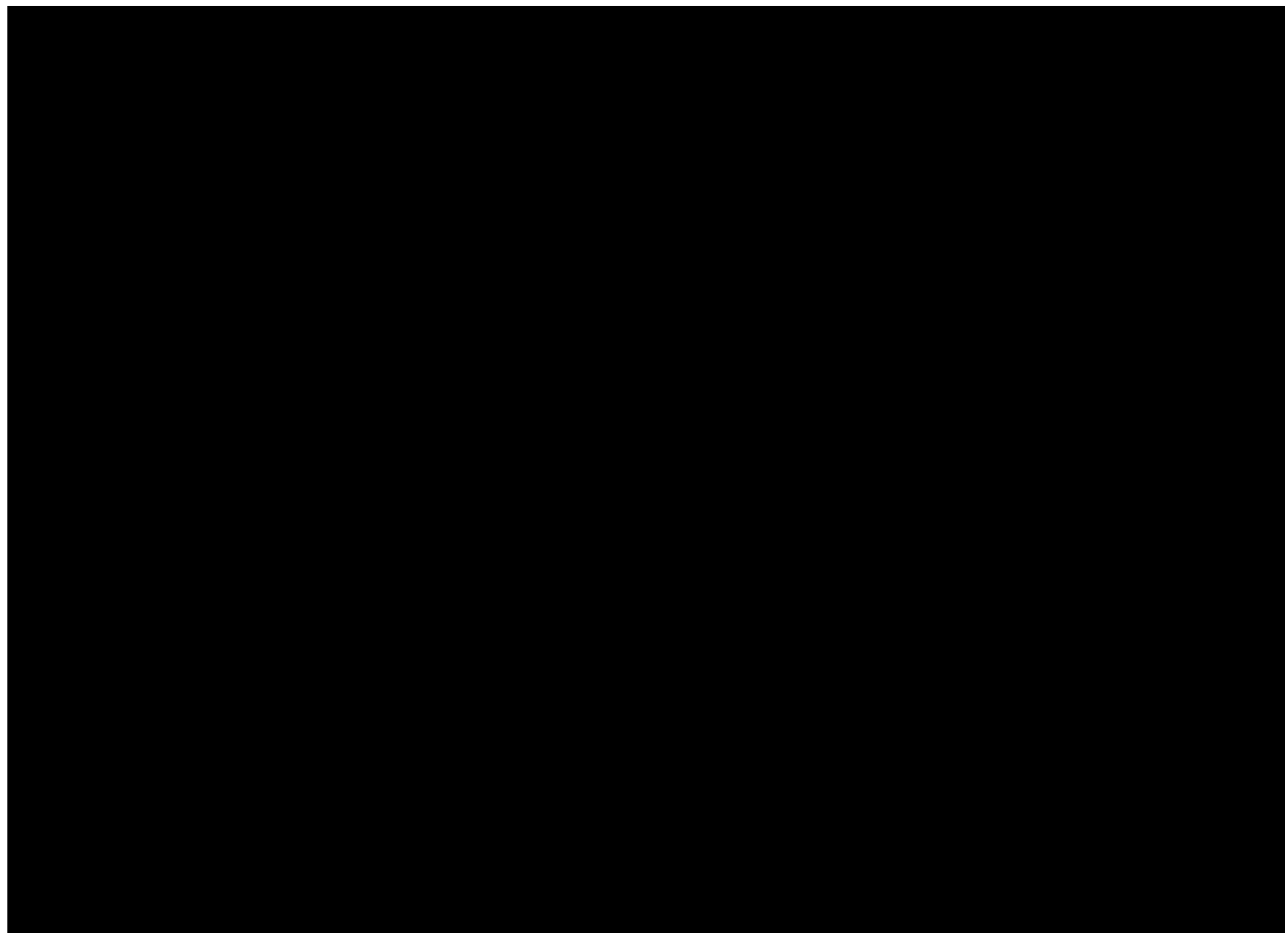


Figure 25. Schematic of Cell Layout and External Heaters for Module Level Test

The unit level test configuration is shown in Figure 26. The module initiating cell was identical to the module level test as shown in Figure 25. The results of the unit level test indicated that one cell was forced into thermal runaway via external heating and one cell entered thermal runaway through thermal runaway propagation. No flaming or flying debris were observed during the unit level test.

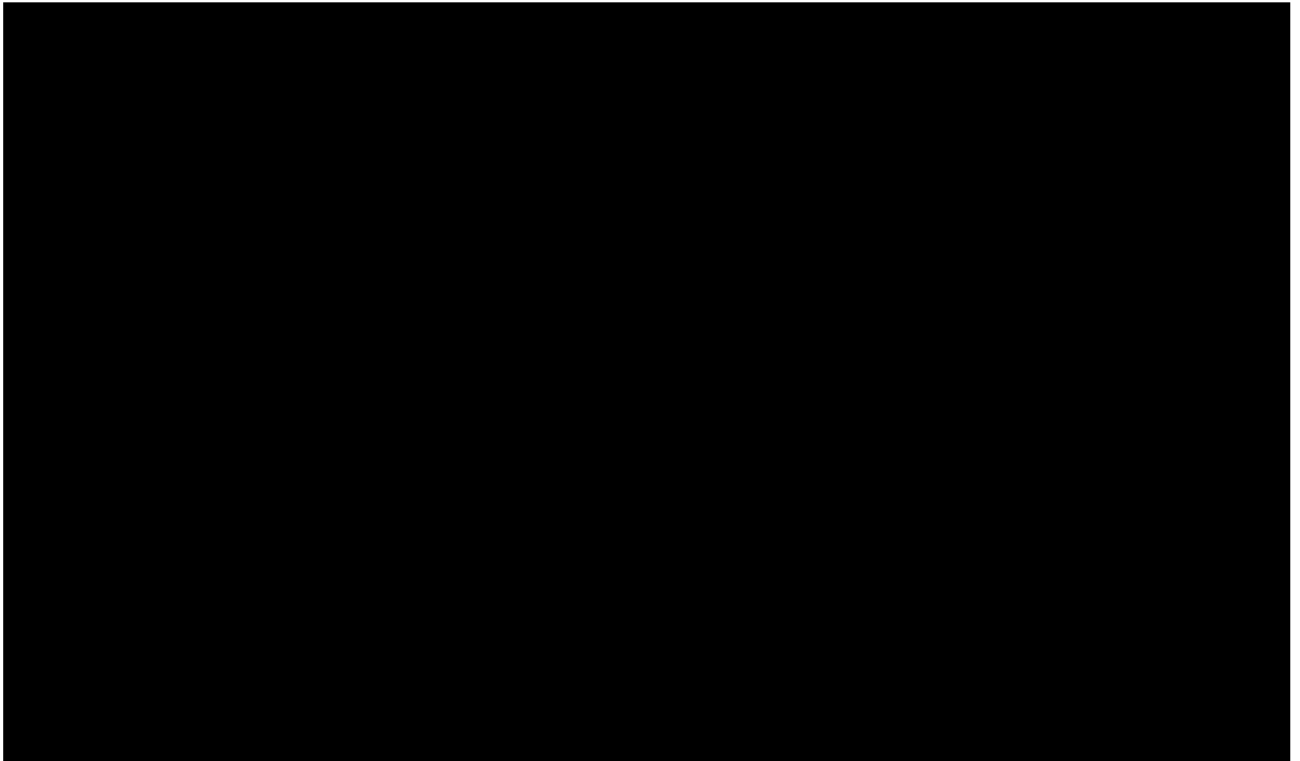


Figure 26. Unit level test setup

C. ADDITIONAL FDS RESULTS**1) SCENARIO 1: EAST WIND RESULTS**

The figures below show the incident heat flux and temperature results for the 25 MPH wind conditions and 50 MPH wind conditions from various locations in the model domain.

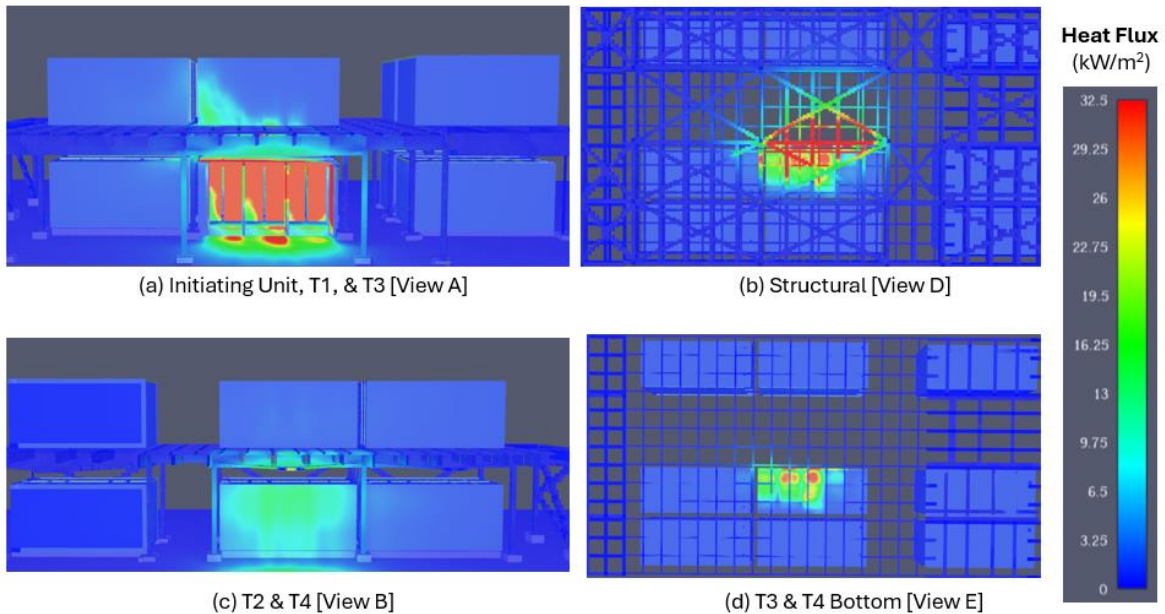


Figure 27. Incident heat flux for 25 MPH wind conditions at (a) View A, (b) View D, (c) View B, (d) View E

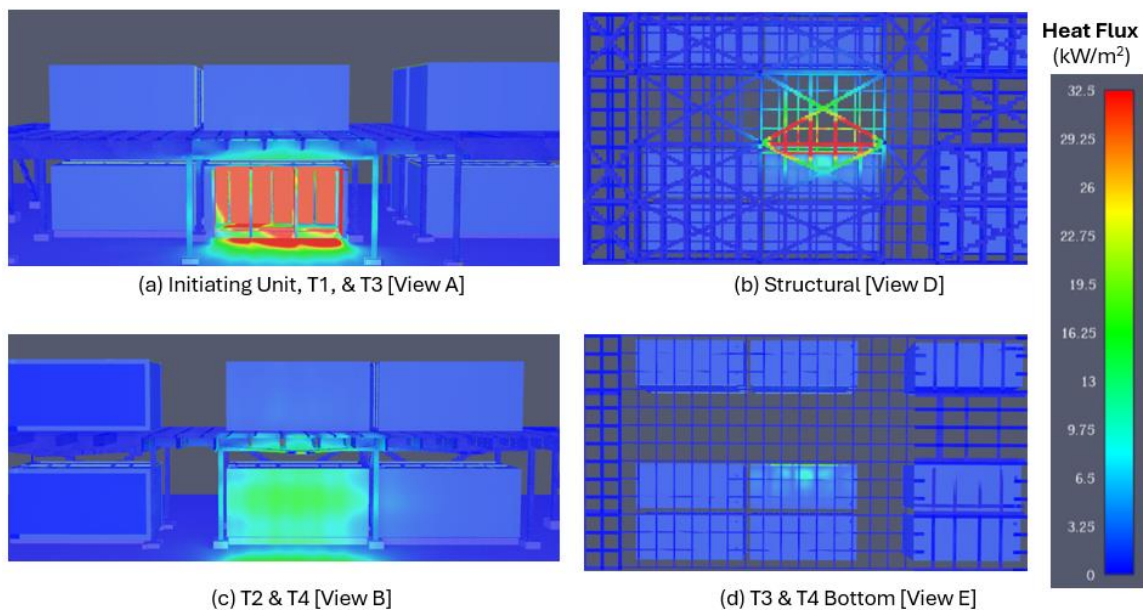


Figure 28. Incident heat flux for 50 MPH wind conditions at (a) View A, (b) View D, (c) View B, (d) View E

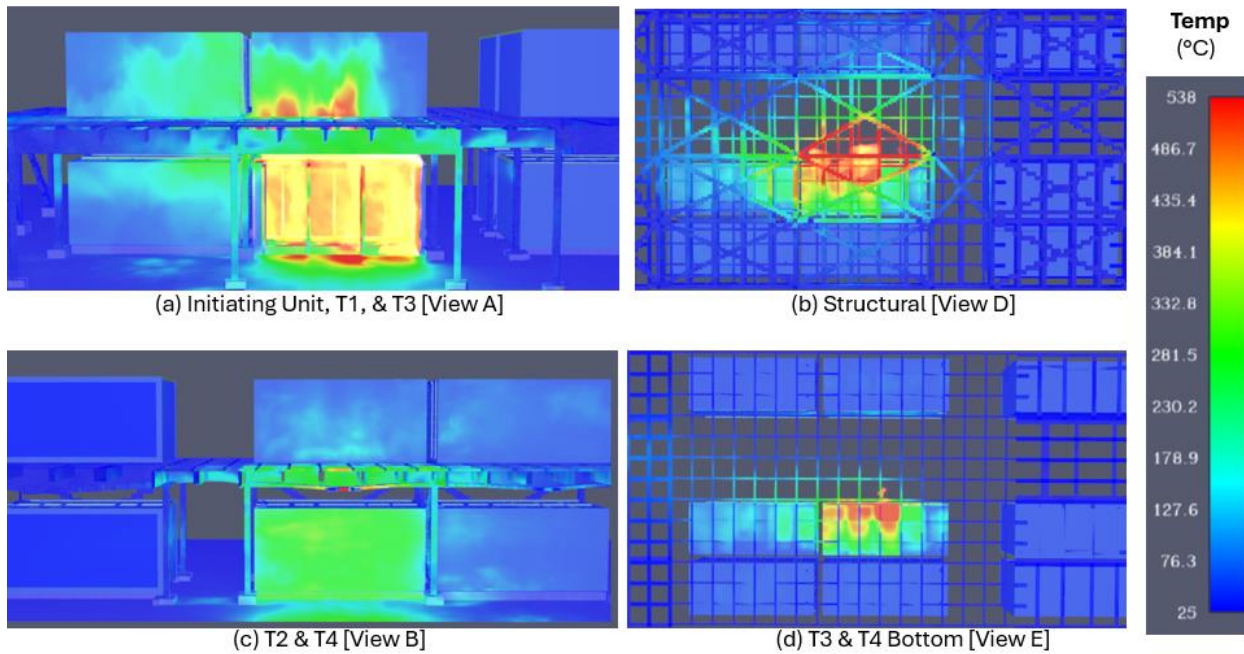


Figure 29. Surface temperature for 25 MPH wind conditions at (a) View A, (b) View D, (c) View B, (d) View E

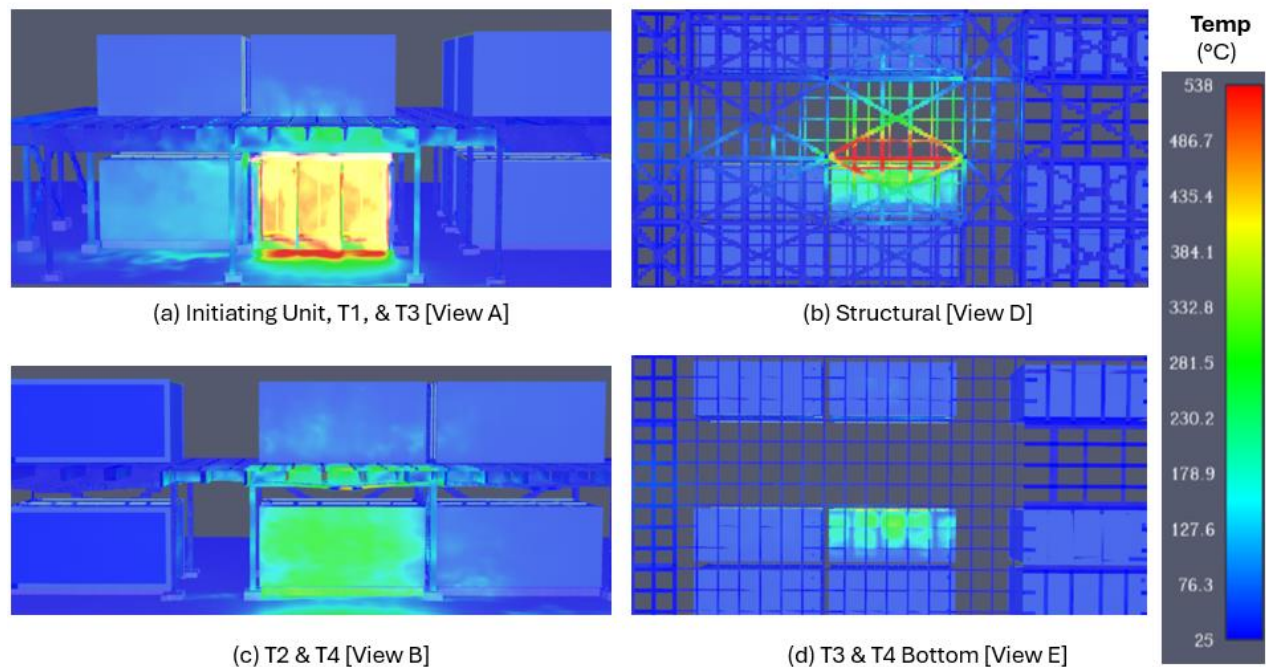


Figure 30. Surface temperature for 25 MPH wind conditions at (a) View A, (b) View D, (c) View B, (d) View E

2) SCENARIO 1: WEST WIND RESULTS

The figures below show the incident heat flux and temperature results for the 25 MPH wind conditions and 50 MPH wind conditions from various locations in the model domain.

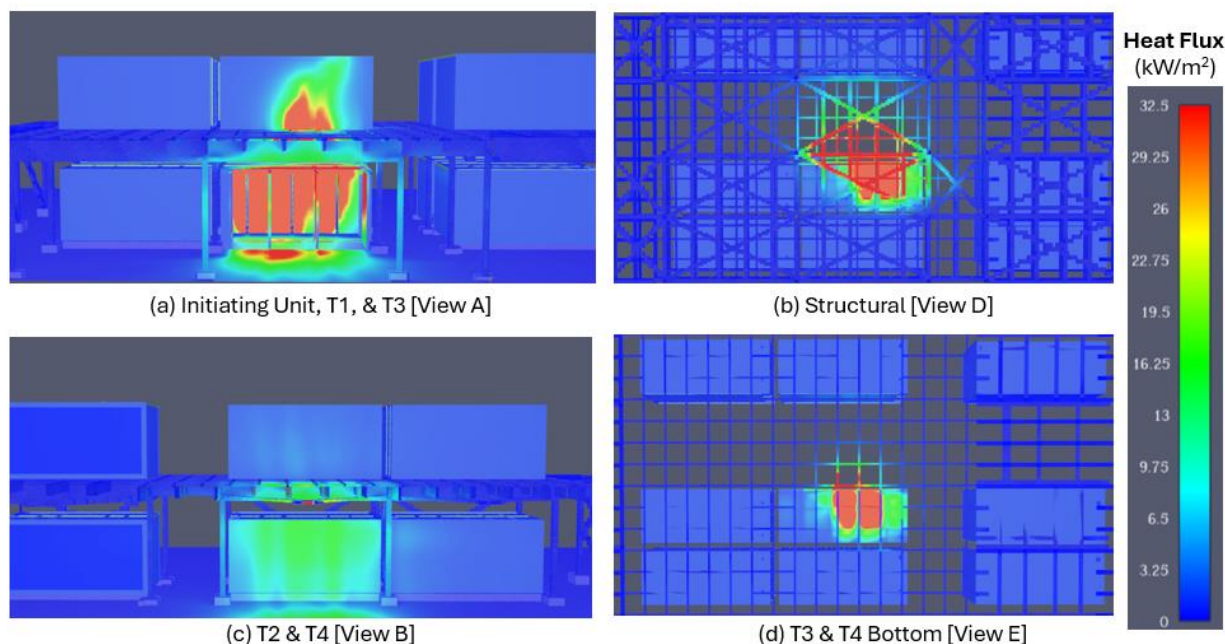


Figure 31. Incident heat flux for 25 MPH wind conditions at (a) View A, (b) View D, (c) View B, (d) View E

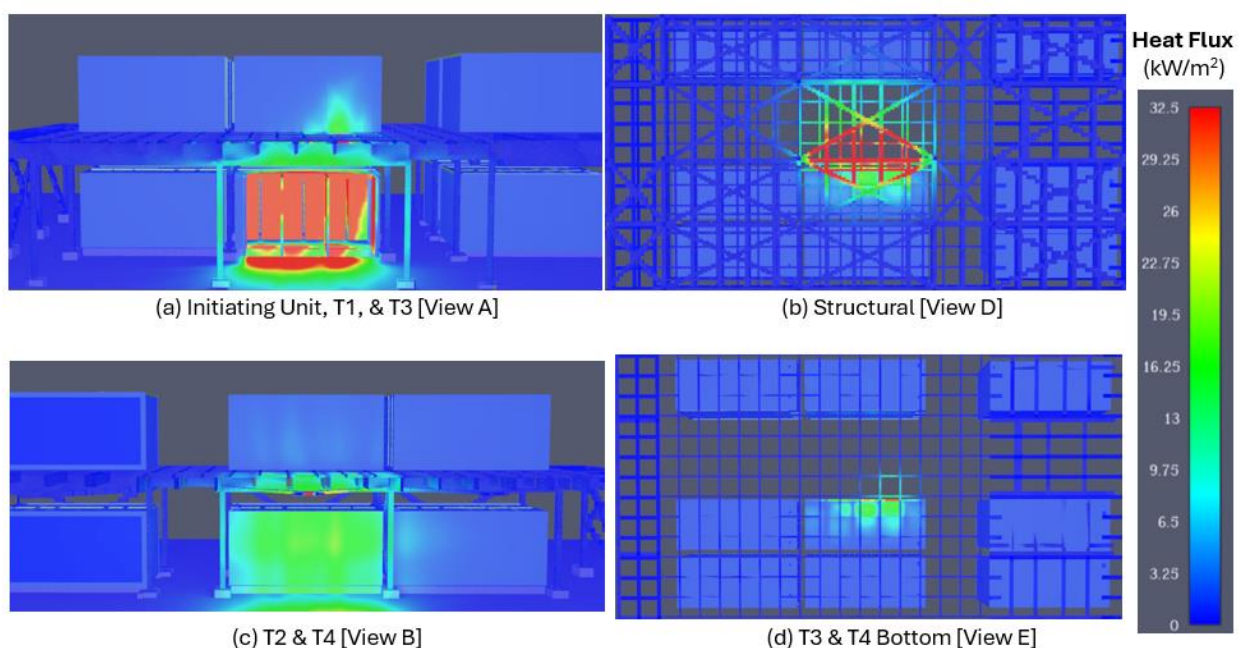


Figure 32. Incident heat flux for 50 MPH wind conditions at (a) View A, (b) View D, (c) View B, (d) View E

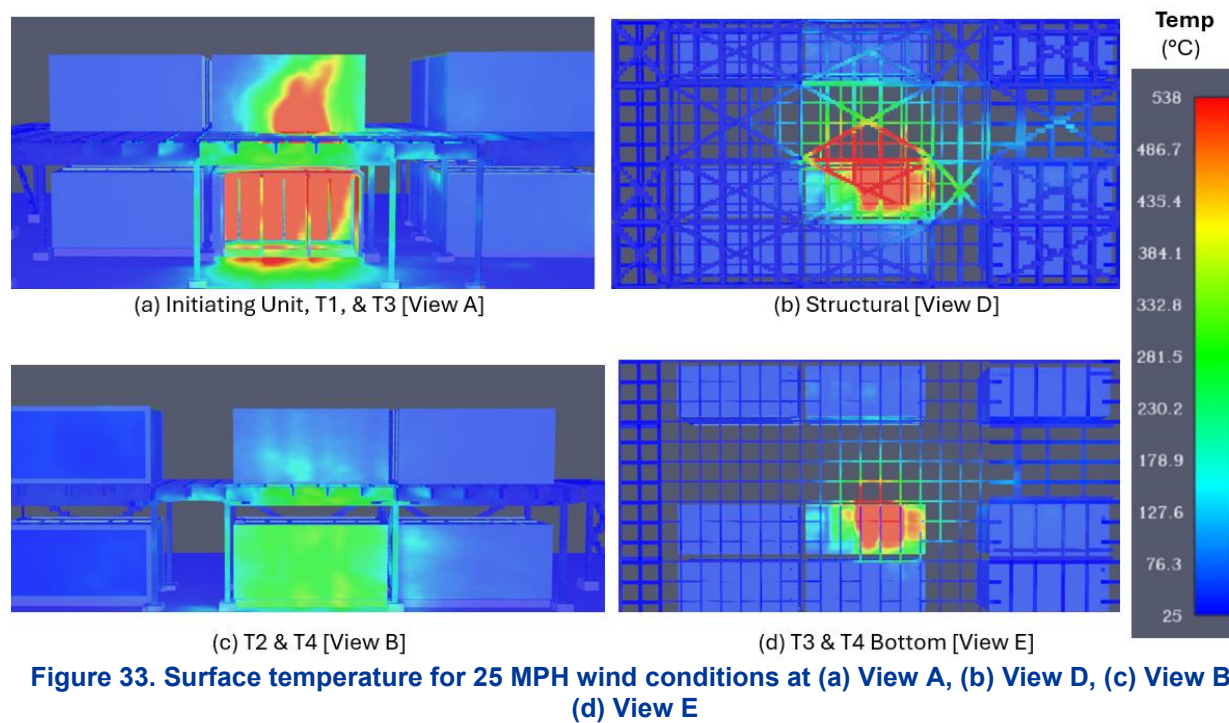


Figure 33. Surface temperature for 25 MPH wind conditions at (a) View A, (b) View D, (c) View B, (d) View E

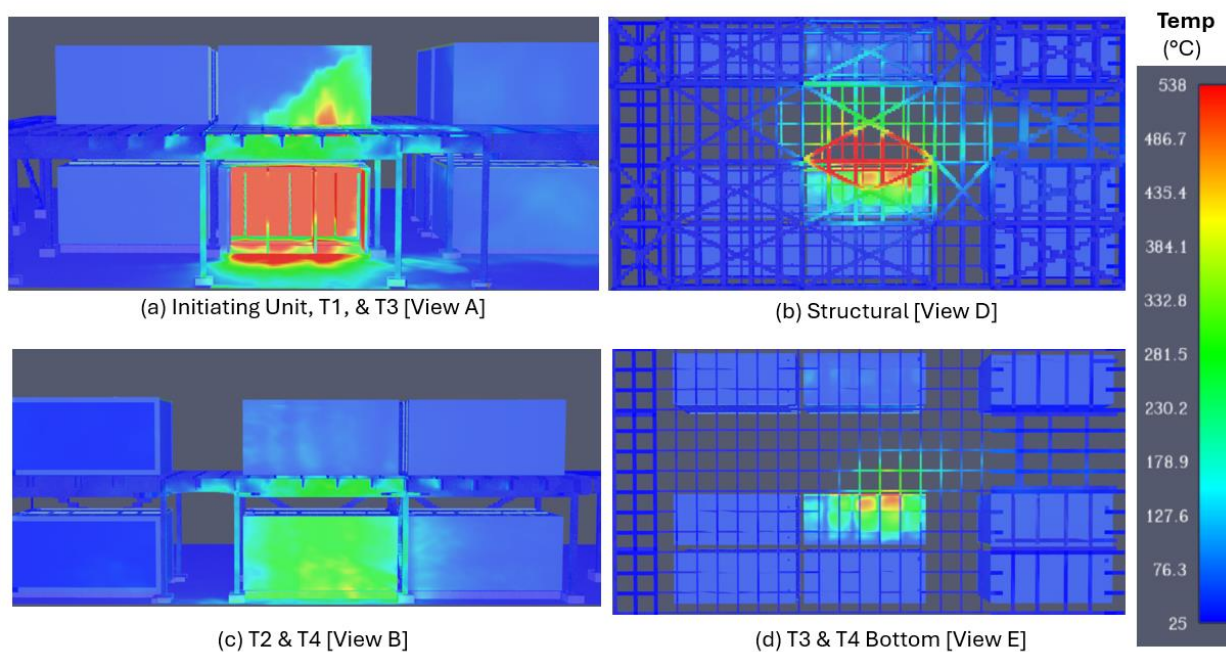


Figure 34. Surface temperature for 25 MPH wind conditions at (a) View A, (b) View D, (c) View B, (d) View E

3) SCENARIO 3: EAST WIND RESULTS

The figures below show the incident heat flux and temperature results for the 25 MPH wind conditions and 50 MPH wind conditions from various locations in the model domain.

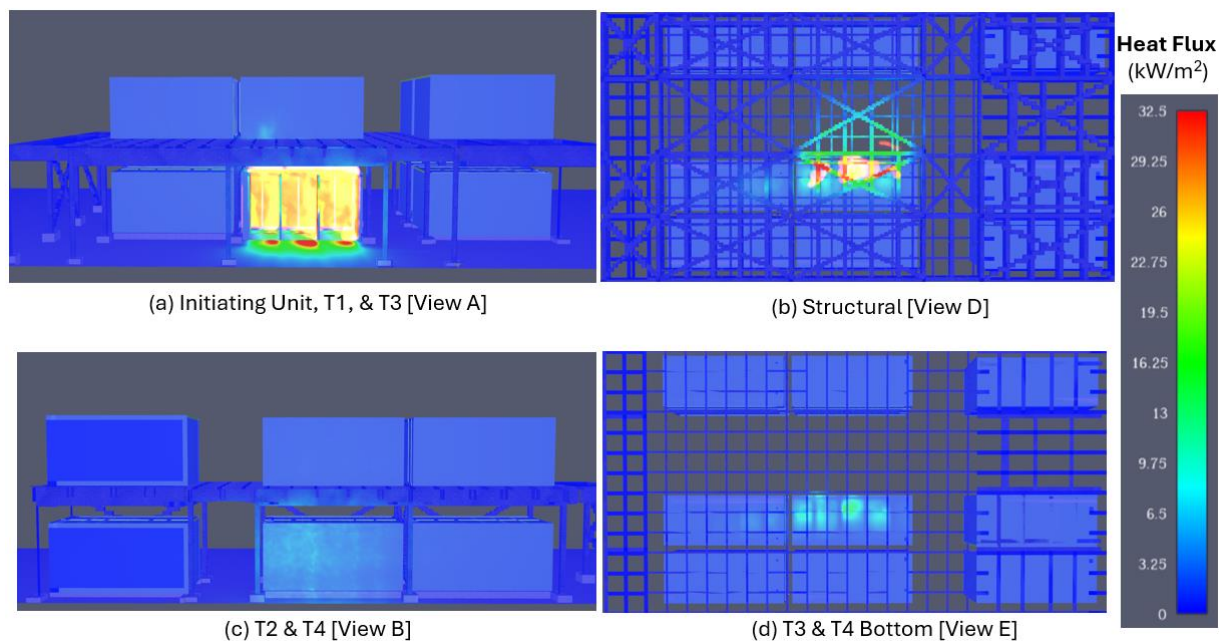


Figure 35. Incident heat flux for 25 MPH wind conditions at (a) View A, (b) View D, (c) View B, (d) View E

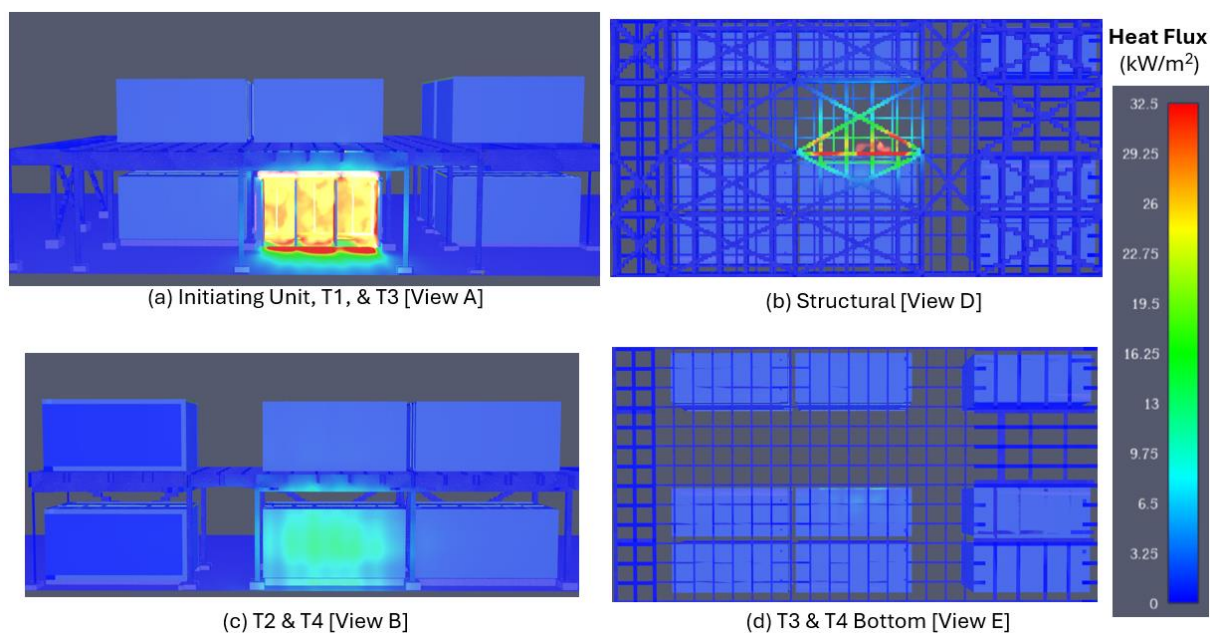


Figure 36. Incident heat flux for 50 MPH wind conditions at (a) View A, (b) View D, (c) View B, (d) View E

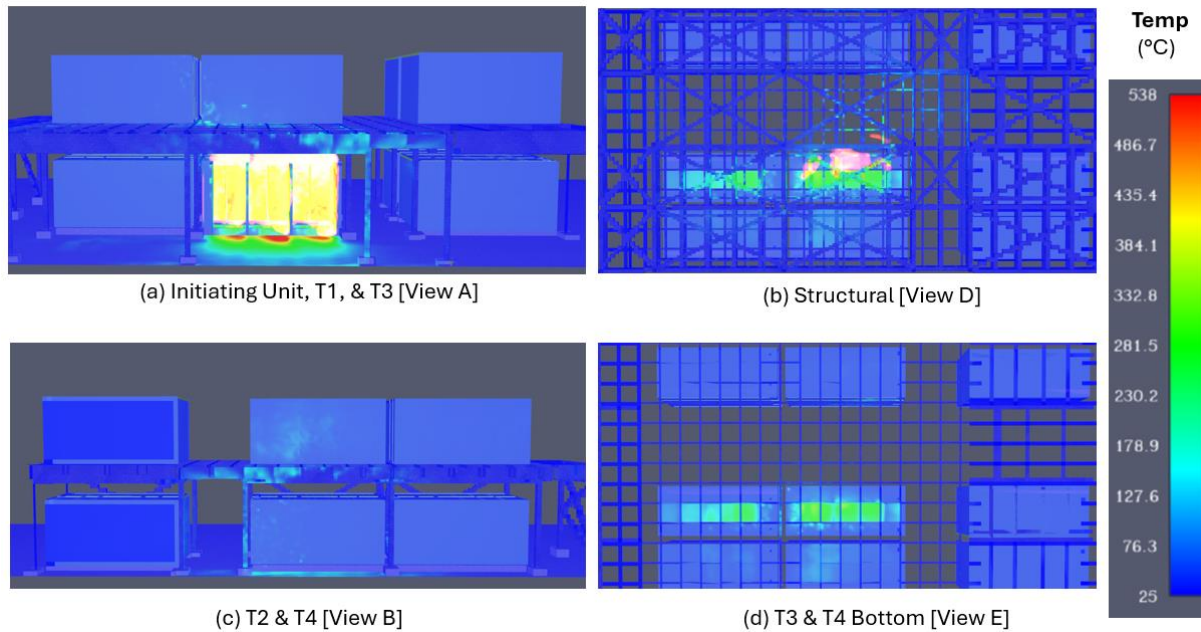


Figure 37. Surface temperature for 25 MPH wind conditions at (a) View A, (b) View D, (c) View B, (d) View E

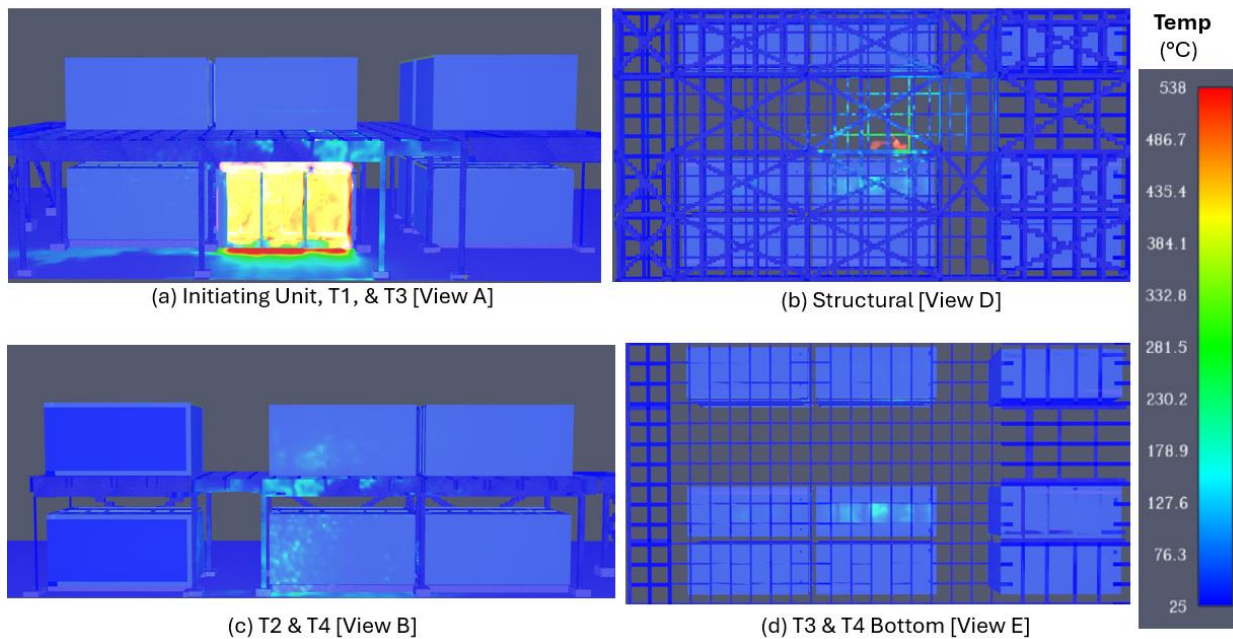


Figure 38. Surface temperature for 25 MPH wind conditions at (a) View A, (b) View D, (c) View B, (d) View E

4) SCENARIO 3: WEST WIND RESULTS

The figures below show the incident heat flux and temperature results for the 25 MPH wind conditions and 50 MPH wind conditions from various locations in the model domain.

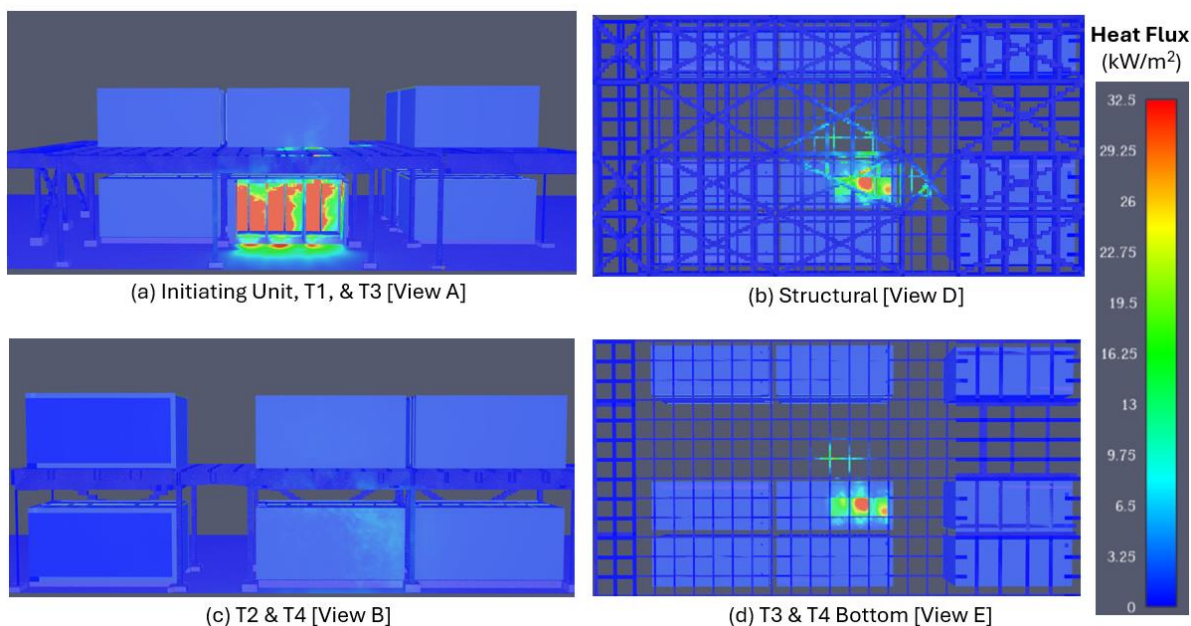


Figure 39. Incident heat flux for 25 MPH wind conditions at (a) View A, (b) View D, (c) View B, (d) View E

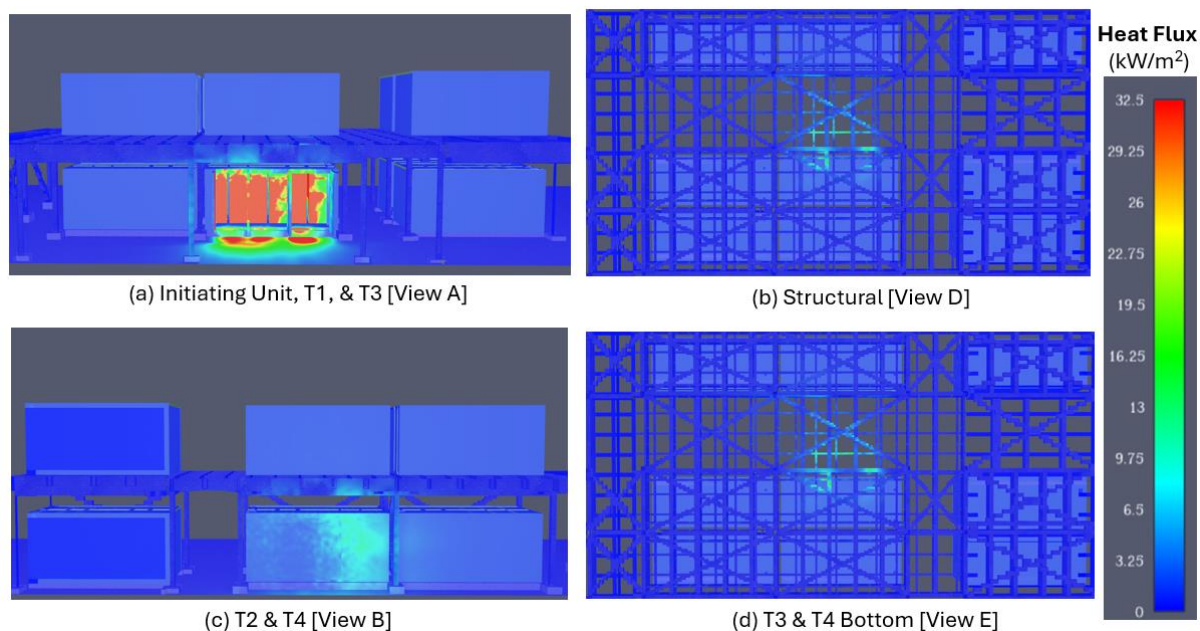


Figure 40. Incident heat flux for 50 MPH wind conditions at (a) View A, (b) View D, (c) View B, (d) View E

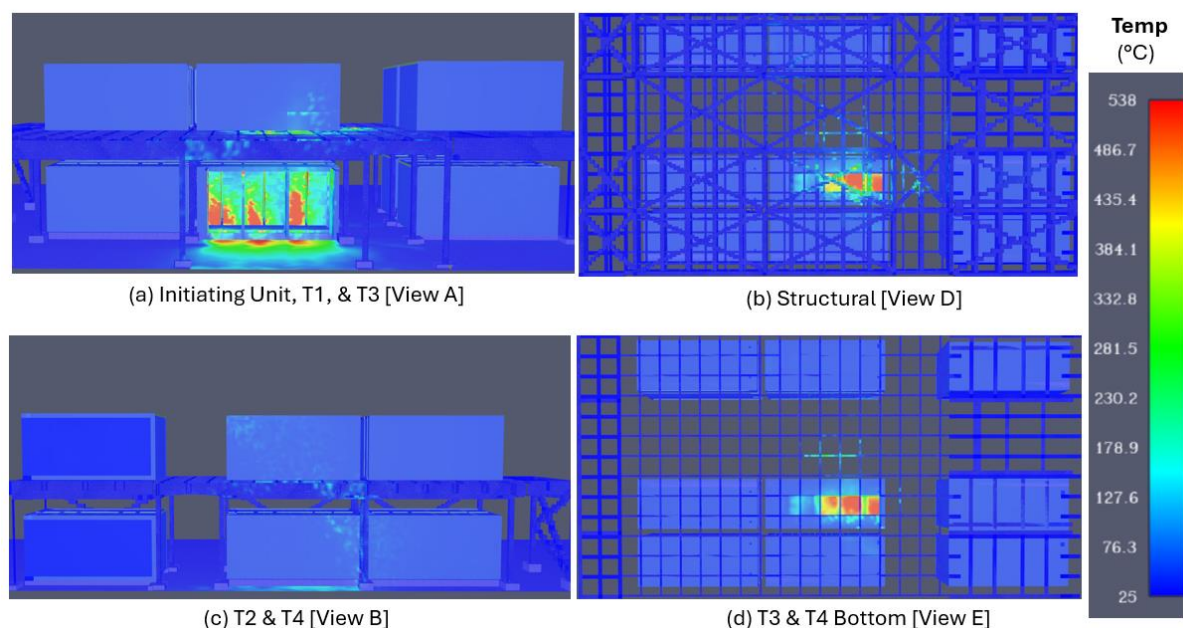


Figure 41. Surface temperature for 25 MPH wind conditions at (a) View A, (b) View D, (c) View B, (d) View E

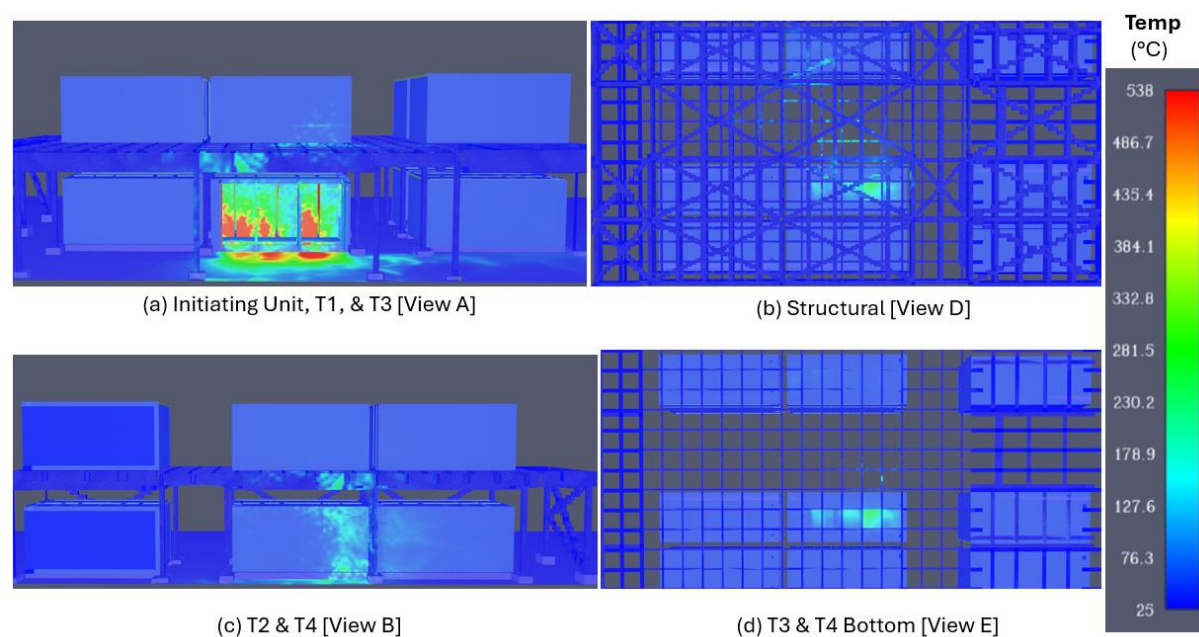


Figure 42. Surface temperature for 25 MPH wind conditions at (a) View A, (b) View D, (c) View B, (d) View E